

FedST: Federated Shapelet Transformation for Interpretable Time Series Classification

Zhiyu Liang
Harbin Institute of Technology
Harbin, China
zyliang@hit.edu.cn

Hongzhi Wang
Harbin Institute of Technology
Harbin, China
wangzh@hit.edu.cn

ABSTRACT

This paper studies how to develop accurate and interpretable time series classification (TSC) models with the help of external data in a privacy-preserving federated learning (FL) scenario. To the best of our knowledge, we are the first to study on this essential topic. Achieving this goal requires us to seamlessly integrate the techniques from multiple fields including Data Mining, Machine Learning, and Security. In this paper, we formulate the problem and identify the interpretability constraints under the FL setting. We systematically investigate existing TSC solutions for the centralized scenario and propose FedST, a novel FL-enabled TSC framework based on a shapelet transformation method. We recognize the federated shapelet search step as the kernel of FedST. Thus, we design FedSS-B, a basic protocol for the FedST kernel that we prove to be secure and accurate. Further, we identify the efficiency bottlenecks of the basic protocol and propose optimizations tailored for the FL setting for acceleration. Our theoretical analysis shows that the proposed optimizations are secure and more efficient. We conduct extensive experiments using both synthetic and real-world datasets. Empirical results show that our FedST solution is effective in terms of TSC accuracy, and the proposed optimizations can achieve three orders of magnitude of speedup.

PVLDB Reference Format:

Zhiyu Liang and Hongzhi Wang. FedST: Federated Shapelet Transformation for Interpretable Time Series Classification. PVLDB, 14(1): XXX-XXX, 2020.
doi:XX.XX/XXX.XX

PVLDB Artifact Availability:

The source code, data, and/or other artifacts have been made available at URL_TO_YOUR_ARTIFACTS.

1 INTRODUCTION

Time series classification (TSC) aims to predict the class label for given time series samples. It is one of the most important techniques for data analytics, with many applications in various scenarios [25, 28, 44, 77, 81]. Numerous algorithms [2, 7, 8, 26, 40, 67, 78, 82, 83] have been proposed to address this problem.

Despite the impressive performance these methods have been achieving, existing methods make an ideal assumption that the user has free access to enough labeled data. However, it is quite difficult

to collect and label the time series for real-world applications. For instance, small manufacturing businesses monitor their production lines using sensors to analyze the working condition. Since the segment related to specific conditions, e.g., a potential failure of an instrument, are usually rare pieces located in unknown regions of the whole monitoring time series, the users have to manually identify the related pieces for labeling, which can be expensive due to the need of professional knowledge. As a consequence, it is costly for these businesses to benefit from the advanced TSC solutions, as they have no enough labeled data to learn accurate models. To deal with the problem, a natural idea is to enrich the local training data by gathering the labeled samples from external data sources, e.g., the other businesses that run the same instrument. However, it has been increasingly difficult for organizations to combine their data due to privacy concerns [86, 91].

Is it possible to build accurate TSC models with the help of external datasets in a privacy-preserving manner? A recent concept, named *Federated Learning* (FL) [41, 49, 60, 62, 91, 96], provides us an inspiration. FL aims to enable multiple businesses to jointly train a model without revealing their private data to each other. Unfortunately, existing FL solutions fail to tackle the TSC problem for two reasons. First, while existing FL works have focused on training standard classification models such as tree models [3, 21, 30, 31, 50, 89], linear models [5, 18, 69, 73, 92], and neural networks [1, 13, 32, 62–64, 79], it has been proved that most of these standard classifiers cannot achieve satisfactory TSC accuracy because the latent temporal features may be dismissed [8]. Second, many real-world TSC applications [25, 33, 75, 77, 90, 94] expect the methods to be interpretable, e.g., the users know why a working condition is determined as a fault, but no existing FL method considers this issue.

The above limitations motivate us to *enable interpretable TSC based on FL*. In specific, we target the setting where a business (named initiator) collaborates with a few partners (named participants) to jointly train a TSC model over their private training samples while the model is locally used by the initiator for prediction. The setting is similar to the *horizontal* and *cross-silo* FL [41, 60], but is more practical and challenging since i) we need to ensure that the classification decision is explainable; ii) we remove the dependency on a trusted server; iii) we adopt a stronger security model for privacy protection. To the best of our knowledge, we are the first to investigate the above problem. To deal with it, a direct idea is to adapt state-of-the-art centralized TSC methods to the FL scenario, which can be lossless in terms of classification accuracy. However, we highlight two major challenges for this solution.

First, to guarantee the FL security, a commonly used method is to leverage secure multi-party computation (MPC) [23, 42, 43, 93] that enables the parties (businesses) to collaboratively compute any function without privacy leakage. Unfortunately, the direct

This work is licensed under the Creative Commons BY-NC-ND 4.0 International License. Visit <https://creativecommons.org/licenses/by-nc-nd/4.0/> to view a copy of this license. For any use beyond those covered by this license, obtain permission by emailing info@vldb.org. Copyright is held by the owner/author(s). Publication rights licensed to the VLDB Endowment.
Proceedings of the VLDB Endowment, Vol. 14, No. 1 ISSN 2150-8097.
doi:XX.XX/XXX.XX

adaption of the centralized TSC methods can be inefficient, because it incurs high communication overhead with the execution of abundant MPC operations. Second, the explanation of the centralized TSC methods could be insecure in the FL setting. For example, consider one of the most popular TSC baselines, the one nearest neighbor (1NN) using dynamic time wrapping (DTW) [8, 11, 78], which predicts the label as the same as the sample queried from the training database that has the minimum DTW distance to the predicted sample. To explain the 1NN classifier in the FL setting, a party has to access the retrieved raw time series. It means that the private data of other parties, when being the 1NN query answer, has to be revealed, which undoubtedly violates the data privacy.

To cope with the above problems, we propose to *specifically design interpretable TSC methods* that achieve a good balance among *security, accuracy, as well as efficiency*. To achieve this goal, we first identify the general *constraints* that guarantee both security and interpretability under the FL setting. Then, we propose to design TSC algorithms that not only satisfy these constraints, but also perform well in terms of accuracy and efficiency. In particular, following the design consideration of interpretability, accuracy and flexibility, as discussed in Section 4.1, we propose a novel FL-enabled TSC framework based on the centralized shapelet transformation method [7, 14]. We identify the *federated shapelet search (FedSS)* step as the kernel of the framework, which brings challenges in terms of privacy preservation and efficiency. Thus, we design specific security protocols to tackle these issues.

To tackle the security issue, we first present a basic protocol $\Pi_{FedSS-B}$, which directly extends the centralized shapelet search using secure multi-party computation (MPC) [23, 42, 43, 93] for privacy protection. We show that this protocol is secure and effective. However, this extension suffers from low efficiency due to the high communication overhead incurred by MPC during the *shapelet distance computation* and the *shapelet quality measurement* stages. Moreover, while there are acceleration techniques for the centralized method [45, 71, 76, 94], we prove that these methods are insecure in the FL setting and thus to be unfeasible.

To overcome the low efficiency of $\Pi_{FedSS-B}$, we further propose *acceleration techniques tailored for the FL setting* to tackle the two bottlenecks. For shapelet distance computation, we propose to speed up the bottlenecked Euclidean distance computation based on a novel secure dot-product protocol. For quality measurement, we first propose an optimization to reduce the duplicated time-consuming interactive operations based on secure sorting. Then, we propose a method to further boost the efficiency through an acceptable trade-off of classification accuracy. We show both theoretically and empirically the effectiveness of these techniques.

Contributions. We summarize our contributions as follows.

- We are the first to study how to enable FL for interpretable TSC. We formally define the new problem and identify the interpretability constraints in the FL setting, and we propose Federated Shapelet Transformation (FedST), the first FL-enabled TSC solution that tackles the problem.
- We present $\Pi_{FedSS-B}$, a basic protocol for the FedST kernel, i.e., the federated shapelet search, which extends the centralized method using MPC. We analyze the protocol in terms of security, effectiveness, and efficiency.
- We identify the efficiency bottlenecks of $\Pi_{FedSS-B}$. To overcome these bottlenecks, we propose acceleration techniques

tailored for the FL setting to significantly boost the protocol efficiency.

- We conduct extensive experiments to evaluate our solution, which has three major observations. i) Our FedST offers superior accuracy comparable to the non-private approach. ii) Each of our proposed acceleration techniques is individually effective, and these techniques together bring up to three orders of magnitude of speedup. iii) The proposed trade-off method achieves up to 8.31x of speedup over our well-optimized solution while guaranteeing comparable accuracy. We further demonstrate the interpretability and flexibility of our framework.

2 PROBLEM FORMULATION

Time series classification (TSC) is the problem of creating a function that maps from the space of input series to the space of class labels [8]. The time series is defined as a sequence of observations $T = (t_1, \dots, t_p, \dots, t_N)$ ordered by time, where t_p is the observation at timestamp p , and N is the length. The class label y is a discrete variable with C possible values. i.e., $y \in \{c_i\}_{i=1}^C$ where $C \geq 2$. TSC is achieved by using a training dataset $TD = \{(T_j, y_j)\}_{j=1}^M$ to build a model that can output either predicted class values or class distributions for previously unseen series, where the instance (T_j, y_j) represents the pair of the j -th series and the corresponding label.

Specifically, we target an FL setting that a party (business) P_0 who owns a training data set TD^0 aims to build a TSC model to predict the unseen local data, with the help of $n-1$ partners P_1, \dots, P_{n-1} who hold the labeled series TD^1, \dots, TD^{n-1} collected from the same area (e.g., monitoring the same type of instruments), where $TD^i = \{(T_j^i, y_j^i)\}_{j=1}^{M_i}$. The n parties must guarantee no private data is revealed to each other. *Note that every party in the group can serve as the initiator to benefit from the federated learning.* For ease of exposition, we denote $\sum_{i=0}^{n-1} M_i = M$ and $\bigcup_{i=0}^{n-1} TD^i = TD$.

The setting is similar to the horizontal and cross-silo FL [41, 60] because the data are horizontally partitioned across a few businesses. However, our setting is more practical but challenging. First, while the primary goal of TSC is to achieve high classification accuracy, most real-world applications, such as fault detection and electrocardiogram monitoring, require the classification decisions understandable [25, 33, 75, 77, 90, 94]. Therefore, we need the TSC method explainable to the user who initiates the FL, i.e., P_0 . Second, unlike many existing solutions that rely on a trust server [38, 61, 95], we remove this dependency since identifying such a party can cause additional costs [59]. Finally, we adopt a stronger security model for better privacy protection.

We identify the interpretability constraints and the security definition in Section 2.1 and Section 2.2, respectively. Then, we formulate our studied problem, the FL-enabled TSC, in Section 2.3.

2.1 Interpretability constraints

Although explaining a model is quite a challenging problem with many mysteries [6, 29], it is out of the scope of this paper how to explain a model well. In contrast, we focus on a more essential problem which is *how a model trained from FL can be "at least" interpretable for P_0* . Generally, any ML method can be explained, either intrinsically or by adopting post-hoc techniques, if and only if the feature used for explanation is human-understandable [70]. For example, an explanation that 'an image is predicted as a zebra since it shows a feature of strips' is interpretable, but if the feature

is some pixels or output of complex operations that are not human-understandable, the prediction related to the feature will be also incomprehensible [70]. Thus, to *guarantee interpretability* for P_0 , the FL methods need to ensure the following **constraints**:

- C1: The features used for prediction is human-understandable;
- C2: The features can be accessed by P_0 without data leakage.

2.2 Security definition

To avoid data leakage, the parties have to follow *security protocols* Π for computation. Similar to previous FL works [31, 32, 53, 85, 89], we consider the semi-honest model where each party follows the protocols but may try to infer the private information from the received messages. Unlike existing FL works that usually allow revealing some intermediate information, we adopt a stronger security model [69, 89] to ensure *no intermediate information is disclosed*.

DEFINITION 1 (SECURITY PROTOCOL). *A protocol Π securely realizes a functionality \mathcal{F} if for each adversary \mathcal{A} attacking the real interaction, there exists a simulator \mathcal{S} attacking the ideal interaction, such that for all environments \mathcal{Z} , the quantity $|\Pr(\text{REAL}(\mathcal{Z}, \mathcal{A}, \Pi, \lambda) = 1) - \Pr(\text{IDEAL}(\mathcal{Z}, \mathcal{S}, \mathcal{F}, \lambda) = 1)|$ is negligible (in λ).*

Intuitively, the simulator \mathcal{S} must achieve the same effect in the ideal interaction as the adversary \mathcal{A} achieves in the real interaction.

2.3 Our Problem: FL-enabled Interpretable TSC

Based on the above discussions, we define the problem that we target, *FL-enabled interpretable TSC*, as follows.

DEFINITION 2 (FL-ENABLED INTERPRETABLE TSC). *Given a party P_0 (named as initiator) and its partners P_1, \dots, P_{n-1} (named as participants). The goal is to design security protocols that coordinate the parties to build TSC models for P_0 over their local data $TD^0, TD^1, \dots, TD^{n-1}$, while guaranteeing that the interpretability constraints C1 and C2 are satisfied.*

3 PRELIMINARIES

3.1 Shapelet Transformation

Time series shapelets are defined as representative subsequences that discriminates the classes. Denote $S = (s_1, \dots, s_L)$ a shapelet generated from $TD = \{(T_j, y_j)\}_{j=1}^M$ and the length of T_j is N , where $L \leq N$. Let $T_j[s, l]$ denote the subseries of $T_j = (t_{j,1}, \dots, t_{j,N})$ that starts at the timestamp s and has length l , i.e., $T_j[s, l] = (t_{j,s}, \dots, t_{j,s+l-1})$ where $1 \leq s \leq N - l + 1$, the distance between the shapelet and the j -th time series is defined as the minimum Euclidean norm between S and the L -length subseries of T_j , i.e.,

$$d_{T_j, S} = \min_{p \in \{1, \dots, N-L+1\}} \|S - T_j[p, L]\|^2. \quad (1)$$

By definition, $d_{T_j, S}$ reflects the similarity between a localized shape of T_j and S , which is a class-specific feature. The quality of S can be measured by computing the distances to all series in TD , i.e., $D_S = \{d_{T_j, S}\}_{j=1}^M$, and evaluating the differences in distribution of the distances between class values $\{y_j\}_{j=1}^M$. The state-of-the-art method of shapelet quality measurement is to use the *Information Gain (IG)* with a *binary strategy* [14]. Each distance $d_{T_j, S} \in D_S$ is considered as a splitting threshold, denoted as τ . The threshold is used to partition the dataset D_S into $D_S^{\tau, L}$ and $D_S^{\tau, R}$, such that $D_S^{\tau, L} = \{d_{T_j, S} | d_{T_j, S} \leq \tau\}_{j=1}^M$ and $D_S^{\tau, R} = D_S \setminus D_S^{\tau, L}$. The quality of S

is the maximum information gain among the thresholds, i.e.,

$$Q_{IG}(S) = \max_{\tau} H(D_S) - (H(D_S^{\tau, L}) + H(D_S^{\tau, R})), \quad (2)$$

where $H(D) = -(p \log_2 p + (1-p) \log_2 (1-p))$, $p = \frac{|D_{y(S)}|}{|D|}$ is the fraction of samples in D that belongs to the class of the sample generating S , i.e., $y(S) \in \{c_i\}_{i=1}^C$, and $D_{y(S)} = \{d_{T_j, S} | y_j = y(S)\}_{j=1}^M$.

In shapelet transformation, a set of candidates are randomly sampled from the possible subsequences of TD . After measuring the quality of all candidates, the K subsequences with the highest quality are chosen as the shapelets, which are denoted as $\{S_k\}_{k=1}^K$. The shapelets are used to transform the original dataset TD into a newly tabular dataset of K features, where each attribute represents the distance between the shapelet and the original series, i.e., $D = \{(X_j, y_j)\}_{j=1}^M$ where $X_j = (d_{T_j, S_1}, \dots, d_{T_j, S_K})$. The unseen series are transformed in the same way for prediction. D can be used in conjunction with *any classifier*, such as the well-known intrinsically interpretable decision tree and logistic regression [70].

3.2 Secure Multiparty Computation

Secure multiparty computation (MPC) [93] allows participants to compute a function over their inputs while keeping the inputs private. In this paper, we utilize the *additive secret sharing scheme (ASSS)* for MPC [23] since it offers the basic operations applicable to practical situations [20, 52]. ASSS performs in a field \mathbb{Z}_q for a prime q . We denote a value $x \in \mathbb{Z}_q$ that is additively shared among parties as $\langle x \rangle = \{\langle x \rangle_0, \dots, \langle x \rangle_{n-1}\}$, where $\langle x \rangle_i$ is a random *share* of x hold by party P_i . Suppose x is a private value of P_i . To secretly share x , P_i randomly chooses $\langle x \rangle_j \in \mathbb{Z}_q$ and sends it to P_j ($j \neq i$). Then, P_i sets $\langle x \rangle_i = x - \sum_{j \neq i} \langle x \rangle_j \mod q$. To reconstruct x , all parties reveal their *shares* to compute $x = \sum_{i=0}^{n-1} \langle x \rangle_i \mod q$. For ease of exposition, we omit the modular operation in the rest of the paper.

Under the additive secret sharing scheme, a function $z = f(x, y)$ is computed by using a MPC protocol that takes $\langle x \rangle$ and $\langle y \rangle$ as input and outputs the secret shared $\langle z \rangle$. In this paper, we mainly use the following MPC operations as building blocks: *Addition* ($\langle z \rangle = \langle x \rangle + \langle y \rangle$), *Multiplication* ($\langle z \rangle = \langle x \rangle \cdot \langle y \rangle$), *Division* ($\langle z \rangle = \langle x \rangle / \langle y \rangle$), *Comparison* ($\langle z \rangle = \langle x \rangle < \langle y \rangle : \langle 1 \rangle : \langle 0 \rangle$), and *Logarithm* ($\langle z \rangle = \log_2(\langle x \rangle)$). We refer readers to [4, 10, 16, 17] for the details.

Given the result $\langle b \rangle = \langle x \rangle < \langle y \rangle : \langle 1 \rangle : \langle 0 \rangle$, the smaller one of two values $\langle x \rangle, \langle y \rangle$ can be *securely assigned* to $\langle z \rangle$ by $\langle z \rangle = \langle b \rangle \langle x \rangle + (1 - \langle b \rangle) \langle y \rangle$. Thus, it is trivial to perform the *maximum*, *minimum*, and *top-K* computation for a list of secret shares by sequentially comparing and swapping the adjacent elements in the list using the secure comparison operation and the secure assignment method.

4 SOLUTION OVERVIEW

In this section, we overview our FL-enabled interpretable TSC framework, which is built based on the shapelet transformation framework [7, 14, 37] due to the design consideration in Section 4.1. We provide the framework overview in Section 4.2. Then, we identify the FedST kernel and discuss the technical contributions of this paper in Section 4.3.

4.1 Design Consideration

In summary, this work considers the shapelet transformation as the basis to design FL solution due to the following advantages.

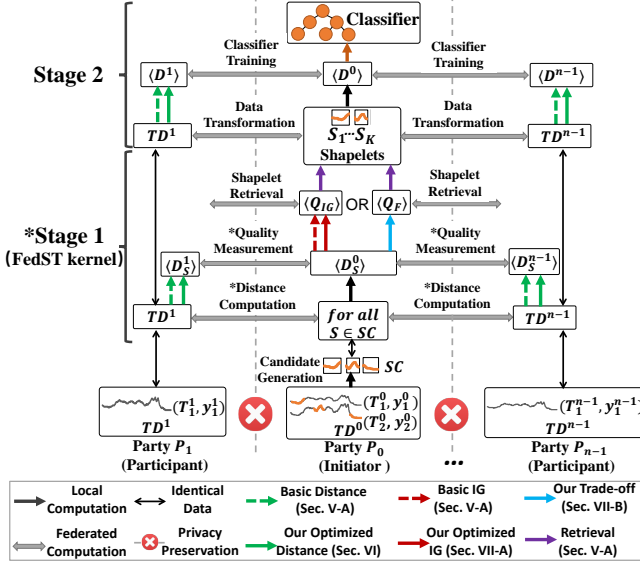


Figure 1: An illustration of the FedST framework.

Interpretable. The shapelet [94] is human-understandable which represents the discriminatory subseries that is close to some classes while far from the others. More importantly, since the high-quality shapelets are usually redundant in the training data, it is enough to find the discriminatory shapelets by checking some randomly sampled candidates, rather than all possible subsequences [7, 35]. Hence, it is feasible to *generate the shapelet candidates from only the training data of the initiator P₀*, while the parties collaboratively select the high-quality shapelets from the candidates. In this way, the user of P₀ can securely explain the classification results using the shapelets since they are local.

Accurate. The shapelet transformation method is one of the state-of-the-art TSC approaches [7, 8, 67]. It can be complementary with other TSC methods through a heterogeneous-feature ensemble to improve the generalization [7, 56, 67].

Flexible. Since the evaluation of each shapelet candidate is in a randomized order and independent from the others, the algorithm can be run in a *contract fashion* [7, 35]. That is, the user announces an expected time such that the algorithm terminates once the running time exceeds, with as many as possible candidates checked. Since the contract relies only on the running time which is public to the parties, it is feasible in the FL setting to flexibly trade off the accuracy and efficiency (see Section 8.5).

4.2 FedST Framework

Based on the above discussions, we propose FedST, *the first FL-enabled interpretable TSC solution* based on shapelet transformation. FedST has two stages: i) federated shapelet search, and ii) federated data transformation and classifier training, as is illustrated in Figure 1. In the first stage, all parties jointly search for the K best shapelets $\{S_k\}_{k=1}^K$ from a candidate set SC generated by the initiator P₀. In stage two, the time series data TD^i in each party is transformed into the K dimensional secretly shared tabular data $\langle D^i \rangle = \{(\langle X_j^i \rangle, \langle y_j^i \rangle)\}_{j=1}^{M_i}$, where $\langle X_j^i \rangle = (\langle d_{T_j^i, S_1}^i \rangle, \dots, \langle d_{T_j^i, S_K}^i \rangle)$. Then, a standard classifier is built over the joint secretly shared dataset $\langle D \rangle = \bigcup_{i=0}^{n-1} \langle D^i \rangle$.

Similar to existing FL works [21, 31, 59], we allow the FL parameters, i.e., the selected shapelets and the classifier to be revealed to P₀ for prediction and explanation, but we ensure no intermediate information is disclosed. The parameters can be further protected such as using differential privacy [53, 74] with the trade-off between security and accuracy/interpretability, which we leave for the future work. The shapelets represent the class-specific shapes of the time series that are highly human-understandable (see Section 8.4). In FedST, the shapelets are generated and used by the same party P₀. Thus, both the constraints in Section 2.1 are satisfied.

4.3 FedST kernel: Federated Shapelet Search

The transformed dataset $\langle D \rangle$ is a common tabular dataset with continuous attributes, which can be used in conjunction with any standard classifier. Consequently, any classifier training protocol built for secretly shared data [3, 20, 69, 97] can be seamlessly integrated into our framework. Nevertheless, there exists no protocol that tackles the orthogonal problem of federated shapelet search and data transformation. Further, the data transformation is to compute the distances between each training series and shapelet, which is just a subroutine of the shapelet search. Thus, the key technical challenge within our FedST is to design secure and efficient protocols to achieve the *federated shapelet search* (Stage 1 in Figure 1), which becomes the kernel part of FedST.

Formally, we define the functionality of the federated shapelet search, \mathcal{F}_{FedSS} , as follows.

DEFINITION 3 (FEDERATED SHAPELET SEARCH, \mathcal{F}_{FedSS}). *Given the time series datasets distributed over the parties, i.e., TD^0, \dots, TD^{n-1} , and the shapelet candidates SC generated from TD^0 , the goal of \mathcal{F}_{FedSS} is to select the K most discriminatory shapelets $\{S_k | S_k \in SC\}_{k=1}^K$ for P₀ by leveraging the distributed datasets.*

To realize \mathcal{F}_{FedSS} under the security defined in Definition 1, a straightforward thought is to design security protocols by extending the centralized method to the FL setting using MPC. Following this, we present $\Pi_{FedSS-B}$ (Section 5.1), the protocol that achieves our basic idea. We show the protocol is *secure* and *effective* (Section 5.2), but we identify that it suffers from *low efficiency* due to the high communication overhead incurred by MPC and the failure of the pruning techniques due to the security issue (Section 5.3). To tackle this issue, we propose *secure acceleration techniques tailored for the FL setting* that dramatically boost the protocol efficiency by reducing the communication cost of the two bottlenecked processes of $\Pi_{FedSS-B}$, i.e., the *distance computation* (Section 6) and the *quality measurement* (Section 7). Experiment results show that each of these techniques is *individually effective* and they together contribute to up to **three orders of magnitude of speedup** (Section 8.3).

5 BASIC PROTOCOL $\Pi_{FedSS-B}$

We now introduce the basic protocol $\Pi_{FedSS-B}$, which is adapted from the centralized shapelet search using MPC to achieve privacy protection (Section 5.1). We discuss the protocol in terms of security, effectiveness, and efficiency in Section 5.2, and analyze the bottlenecks of the protocol in Section 5.3.

5.1 Protocol Description

$\Pi_{FedSS-B}$ is outlined in Algorithm 1. The parties jointly assess the quality of each candidate and then select the K best as the shapelets. The algorithm performs in three steps. First, the parties compute

Algorithm 1: Basic Protocol $\Pi_{FedSS-B}$

Input: $TD^i = \{(T_j^i, y_j^i)\}_{j=1}^{M_i}, i = 0, \dots, n-1$: local datasets
SC: A set of shapelet candidates locally generated by P_0
K: the number of shapelets
Output: $\{S_k\}_{k=1}^K$: shapelets revealed to P_0

```

1 for  $S$  in  $SC$  do
2   for  $i$  in  $\{0, \dots, n-1\}$  do
3     if  $i == 0$  then
4       for  $j$  in  $\{1, \dots, M_0\}$  do
5          $P_0$  locally computes  $d_{T_j^0, S}$  and secretly shares
           the result among all parties
6       else
7         for  $j$  in  $\{1, \dots, M_i\}$  do
8           All parties jointly compute  $\langle d_{T_j^i, S} \rangle$ 
9   All parties jointly compute the quality  $\langle Q_{IG}(S) \rangle$  over
     the secretly shared distances and labels
10  All parties jointly find the  $K$  candidates with the highest
    quality and reveal the indices  $\{\langle I_k \rangle\}_{k=1}^K$  to  $P_0$ 
11 return  $\{S_k = SC_{I_k}\}_{k=1}^K$ 

```

the distance between the samples and each candidate (Lines 2-8). Second, the parties evaluate the quality of the candidate over the secretly shared distances and labels (Lines 9). Finally, the parties jointly retrieve the K candidates with the highest quality and reveal the shares of the indices to P_0 to recover the selected shapelets (Lines 10-11). These three steps are described as follows.

Distance Computation. Since the candidates are locally generated by P_0 , the distance between the samples of P_0 and the candidates can be locally computed. After that, P_0 secretly shares the results to enable the subsequent steps (Lines 3-5).

To compute the distances between the samples of each participant P_i and the candidates (Lines 6-8), the MPC operations have to be adopted. For example, to compute $d_{T_j^i, S}$, P_i and P_0 secretly share T_j^i and S respectively. Next, the parties jointly compute each Euclidean distance $\langle ||S, T_j^i[p, L]||^2 \rangle$ using MPC (see Section 3.2). At last, the parties jointly determine the shapelet distance $\langle d_{T_j^i, S} \rangle$ by Eq. 1 using the secure minimum operation (see Section 3.2).

Quality Measurement. Based on Eq 2, to compute the IG quality of $S \in SC$ (Line 9), we need to securely partition the dataset D_S using each threshold τ and compute the number of samples belonging to each class $c_i, i \in \{1, \dots, C\}$ for $D_S, D_S^{\tau, L}$, and $D_S^{\tau, R}$. We achieve it over the secretly shared distances and labels by leveraging the *indicating vector* defined as follows.

DEFINITION 4 (INDICATING VECTOR). Given a dataset $D = \{x_j\}_{j=1}^M$ and a subset $A \subseteq D$, we define the indicating vector of A , denoted as $\gamma_{A \subseteq D}$, as a vector of size M whose j -th ($j \in \{1, \dots, M\}$) entry represents whether x_j is in A , i.e., $\gamma_{A \subseteq D}[j] = 1$ if $x_j \in A$, and 0 otherwise.

For example, for $D = \{x_1, x_2, x_3\}$ and $A = \{x_1, x_3\}$, the indicating vector of A is $\gamma_{A \subseteq D} = (1, 0, 1)$. Suppose that $\gamma_{A_1 \subseteq D}$ and $\gamma_{A_2 \subseteq D}$ are the indicating vectors of A_1 and A_2 , respectively, we have $\gamma_{A_1 \subseteq D} \cdot \gamma_{A_2 \subseteq D} = |A_1 \cap A_2|$, where $|A_1 \cap A_2|$ is the cardinality of $A_1 \cap A_2$. Specifically, we have $\gamma_{A_1 \subseteq D} \cdot \mathbf{1} = |A_1|$.

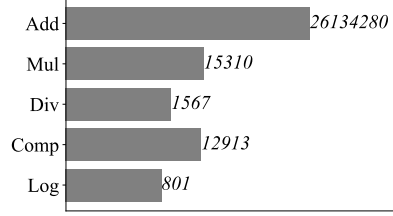


Figure 2: Throughputs (#operations per second) of different MPC operations executed by three parties. Secure addition is much more efficient than the others because it is executed without communication [17].

With the indicating vector, we securely compute $\langle Q_{IG}(S) \rangle$ as follows.

At the beginning, P_0 generates a vector of size C to indicate the class of S , i.e., $\gamma_y(S) = \gamma_{\{y(S)\} \subseteq \{c_i\}_{i=1}^C}$, and secretly shares the vector among all parties. Then, for each splitting threshold $\tau \in \bigcup_{i=0}^{n-1} \{\langle d_{T_j^i, S} \rangle\}_{j=1}^{M_i}$, the parties jointly compute the secretly shared vector $\langle \gamma_L \rangle = \langle \gamma_{D_S^{\tau, L} \subseteq D_S} \rangle$, where $\langle \gamma_{D_S^{\tau, L} \subseteq D_S}[j] \rangle = \langle d_{T_j^i, S} \rangle \stackrel{?}{<} \tau, j \in \{1, \dots, M\}$, and $\langle \gamma_R \rangle = \langle \gamma_{D_S^{\tau, R} \subseteq D_S} \rangle = \mathbf{1} - \langle \gamma_L \rangle$. Meanwhile, each party secretly shares the vector $\gamma_{TD_{c_i}^{\tau, L} \subseteq TD_{c_i}^{\tau, L}}$ to indicate its samples that belong to each class c_i . Denote the indicating vectors of all parties as $\langle \gamma_{c_i} \rangle = (\langle \gamma_{TD_{c_i}^0 \subseteq TD_{c_i}^0} \rangle, \dots, \langle \gamma_{TD_{c_i}^{n-1} \subseteq TD_{c_i}^{n-1}} \rangle)$, which indicates the samples in D_S that belong to class c_i , i.e., $\langle \gamma_{c_i} \rangle = \langle \gamma_{TD_{c_i} \subseteq TD} \rangle = \langle \gamma_{D_S, c_i \subseteq D_S} \rangle$. Therefore, the parties can get $|D_S| = M$, $\langle |D_S^{\tau, L}| \rangle = \langle \gamma_L \rangle \cdot \mathbf{1}$, $\langle |D_S^{\tau, R}| \rangle = |D_S| - \langle |D_S^{\tau, L}| \rangle$ by local computation, and compute the following statistics using MPC:

$$\begin{aligned}
\langle |D_{S, y(S)}| \rangle &= \langle \gamma_y(S) \rangle \cdot (\langle \gamma_{c_1} \rangle \cdot \mathbf{1}, \dots, \langle \gamma_{c_C} \rangle \cdot \mathbf{1}), \\
\langle |D_{S, y(S)}^{\tau, L}| \rangle &= \langle \gamma_y(S) \rangle \cdot (\langle \gamma_{c_1} \rangle \cdot \langle \gamma_L \rangle, \dots, \langle \gamma_{c_C} \rangle \cdot \langle \gamma_L \rangle), \\
\langle |D_{S, y(S)}^{\tau, R}| \rangle &= \langle \gamma_y(S) \rangle \cdot (\langle \gamma_{c_1} \rangle \cdot \langle \gamma_R \rangle, \dots, \langle \gamma_{c_C} \rangle \cdot \langle \gamma_R \rangle).
\end{aligned} \tag{3}$$

Given these statistics, the parties jointly compute $\langle Q_{IG}(S) \rangle$ by Eq. 2. **Shapelet Retrieval.** Given the quality of the candidates in secret shares, the parties jointly retrieve the indices of the K best shapelets (Line 10) by securely comparing the adjacent quality values and swapping the values and the corresponding indices based on the comparison results (see Section 3.2). The indices are output to P_0 to recover the jointly selected shapelets (Line 11).

5.2 Protocol Discussion

This section analyzes $\Pi_{FedSS-B}$ in terms of security, effectiveness, and efficiency.

Security. For the security guarantee of $\Pi_{FedSS-B}$, we have the following Theorem:

THEOREM 1. $\Pi_{FedSS-B}$ is secure under the security model defined in Definition 1.

PROOF SKETCH. In $\Pi_{FedSS-B}$, all joint computations are executed using MPC. With the indicating vector, the secure computations are data-independent. An adversary learns no additional information. The security follows. \square

Effectiveness. We discuss the effectiveness of $\Pi_{FedSS-B}$ in terms of classification accuracy. $\Pi_{FedSS-B}$ is directly extended from the

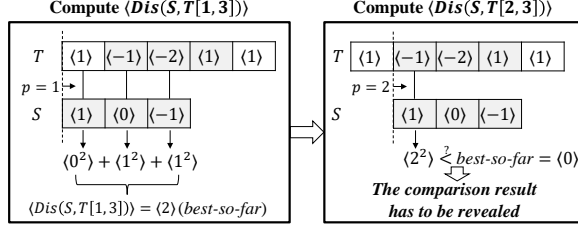


Figure 3: Illustration of the Euclidean distance pruning and its information disclosure.

centralized approach by using the secret-sharing-based MPC operations that have considerable computation precision [4, 16, 17]. Therefore, it is expected that the accuracy of FedST has no difference from the centralized approach. The experiment results in Section 8.2 validate this issue.

Efficiency. As shown in Figure 2, the secret-sharing-based MPC is usually bottlenecked by communication rather than computation. Therefore, it is more indicative to analyze the efficiency by using the complexity of only the *interactive operations*, including the secure multiplication, division, comparison, and logarithm operations. We follow this metric for efficiency analysis in the paper.

$\Pi_{FedSS-B}$ in Algorithm 1 takes $O(|SC| \cdot MN^2)$ for distance computation. The quality measurement has a complexity of $O(|SC| \cdot M^2)$. Securely finding the top- K candidates has a complexity of $O(|SC| \cdot K)$. Since K is usually a small constant, the total complexity of $\Pi_{FedSS-B}$ can be simplified as $O(|SC| \cdot (MN^2 + M^2))$.

5.3 Bottleneck Analysis

As discussed in Section 5.2, $\Pi_{FedSS-B}$ is secure and effective to enable federated shapelet search. However, the basic protocol has expensive time cost in the FL setting for both *distance computation* and *quality measurement* steps, which bottleneck the efficiency of the protocol. Two major reasons are as below.

Reason I. Heavy Communication Overhead. As discussed in Section 5.2, $\Pi_{FedSS-B}$ takes $O(MN^2)$ and $O(M^2)$ expensive interactive operations to compute the distance and measure the quality for each candidate. Note that the number of the candidates $|SC|$ is up to $O(M_0N^2)$ for P_0 . Even though it is never necessary to enumerate all candidates [7, 35], the sampling size $|SC|$ cannot be too small to guarantee that the high-quality shapelets are found for accurate classification. Therefore, the efficiency of $\Pi_{FedSS-B}$ is bottlenecked by the steps of distance computation and quality measurement.

Reason II. Failure of Acceleration Techniques. Even using only local computation, repeatedly computing the distance and quality for abundant candidates are time-consuming [94]. To tackle this, existing studies propose pruning strategies for acceleration [45, 71, 76, 94]. Unfortunately, the pruning techniques are inevitably *data-dependent*, which violates the security of Definition 1 that requires the federated computation oblivious. Thus, we have to abandon these acceleration strategies in the FL setting. We show the security issue in Theorem 2 and Theorem 3.

THEOREM 2. *Protocol $\Pi_{FedSS-B}$ is insecure under the security defined in Definition 1 if using the Euclidean distance pruning strategies proposed in [45] and [76].*

PROOF SKETCH. Figure 3 illustrates the Euclidean distance pruning. The basic idea is to maintain a best-so-far distance and incrementally compute the sum of the squared differences between

each pair of data points (left). Once the sum exceeds the best-so-far distance, the current computation can be pruned (right). In the FL setting, although we can incrementally compute the sum and compare it with the best-so-far distance using MPC, the comparison result must be disclosed when determining the pruning, which cannot be achieved by the simulator \mathcal{S} that attacks the ideal interaction \mathcal{F}_{FedSS} in Definition 3. The security is violated. \square

Similarly, We have the following theorem.

THEOREM 3. *Protocol $\Pi_{FedSS-B}$ is insecure under the security defined in Definition 1 if using the IG quality pruning strategies proposed in [94] and [71].*

We omit the proof because it is similar to the proof of Theorem 2. **Optimization techniques.** To remedy the efficiency issue of the protocol $\Pi_{FedSS-B}$, we propose *acceleration techniques tailored for the FL setting* to improve the efficiency of the distance computation and the quality measurement. For distance computation, we propose to speed up the bottlenecked Euclidean distance computation based on a *novel secure dot-product protocol* (Section 6). For quality measurement, we first propose a *secure sorting-based acceleration* to reduce the duplicated interactive operations IG (Section 7.1). Then, we propose to *tap an alternative F-stat measure* to further improve the efficiency with acceptable loss of accuracy (Section 7.2). Experiment results show that each of these three techniques is individually effective and they together brings up to *three orders of magnitude of speedup* to $\Pi_{FedSS-B}$. Further, compared to our well-optimized IG, the F-stat-based method in Section 7.2 gives 1.04-8.31x of speedup while guaranteeing comparable TSC accuracy. (Section 8.3).

6 SHAPELET DISTANCE ACCELERATION

In $\Pi_{FedSS-B}$, the distance between a candidate S and the $M - M_0$ series of $T_j^i (i \neq 0)$ is straightforwardly computed using MPC. Based on Eq 1, the interactive operations used include: i) $L_S(N - L_S + 1)(M - M_0)$ pairwise multiplications for the Euclidean norm, and ii) $(N - L_S + 1)(M - M_0)$ times of both comparisons and assignments for the minimum. Because the shapelet length L_S is up to $N \gg 1$, the communication overhead is dominated by the Euclidean norm. Thus, it is necessary to accelerate the distance computation by improving the efficiency of the bottlenecked *Euclidean norm*.

The work of [39] proposes a two-party dot-product protocol (as Algorithm 2) that we find is both computation and communication efficient for the calculation between one vector and many others. It motivates us that we can compute the Euclidean distances between a candidate S and the total $(N - L_S + 1)(M - M_0)$ subseries of the participants using the dot-product protocol. Unfortunately, the protocol in Algorithm 2 (denoted as the raw protocol) has weak security that violates Definition 1. To overcome the limitation, we propose Π_{DP} , a *secure dot-product protocol* that enhances the raw protocol using MPC. We prove that this novel protocol not only follows the security of Definition 1, but also effectively accelerates the Euclidean distance. We describe the acceleration method in Section 6.1. Then, we analyze the security deficiency of the raw protocol and propose our Π_{DP} in Section 6.2.

6.1 Dot-Product-based Euclidean Distance

Given two vectors $\mathbf{x} \in \mathbb{R}^L$ from P_0 and $\mathbf{y} \in \mathbb{R}^L$ from P_i , Algorithm 2 computes the dot-product $\mathbf{x} \cdot \mathbf{y}$ as: **1)** P_0 chooses a random matrix $\mathbf{Q} \in \mathbb{R}^{d \times d} (d \geq 2)$, a random value $r \in \{1, \dots, d\}$, a random vector $\mathbf{f} \in \mathbb{R}^{L+1}$ and three random values $R1, R2, R3$, and selects $s - 1$

Algorithm 2: The Two-Party Dot-Product Protocol of [39]

Input: $\mathbf{x} \in \mathbb{R}^L$ from P_0 ; $\mathbf{y} \in \mathbb{R}^L$ from P_i ($i \in \{1, \dots, n-1\}$)

Output: β to P_0 and α to P_i , satisfying $\beta - \alpha = \mathbf{x}^T \cdot \mathbf{y}$

- 1 **Party P_0** randomly chooses $\mathbf{Q}, r, \mathbf{f}, R_1, R_2, R_3, \mathbf{x}_i$ ($i \in \{1, \dots, d\}, i \neq r$) and creates \mathbf{X} . Then, it computes $\mathbf{b}, \mathbf{U}, \mathbf{c}, \mathbf{g}$, and sends $\mathbf{U}, \mathbf{c}, \mathbf{g}$ to P_i
 - 2 **Party P_i** randomly chooses α , creates \mathbf{y}' , computes and sends to P_0 the value a, h
 - 3 **Party P_0** computes β
-

Algorithm 3: Secure Dot-Product Protocol Π_{DP} (Ours)

Input: $\mathbf{x} \in \mathbb{R}^L$ from P_0 ; $\mathbf{y} \in \mathbb{R}^L$ from P_i ($i \in \{1, \dots, n-1\}$)

Output: $\langle z \rangle$ secretly shared by all parties, satisfying $z = \mathbf{x}^T \cdot \mathbf{y}$

- 1 **Party P_0 and Party P_i** represent each element of their input vectors as fixed-point number encoded in \mathbb{Z}_q as used in MPC
 - 2 **Party P_0** independently and randomly chooses each value of $\mathbf{Q}, \mathbf{f}, R_1, R_2, R_3, \mathbf{x}_i$ ($i \in \{1, \dots, d\}, i \neq r$) from \mathbb{Z}_q , $r \in \{1, \dots, d\}$, creates \mathbf{X} , computes $\mathbf{b}, \mathbf{U}, \mathbf{c}, \mathbf{g}$, and sends $\mathbf{U}, \mathbf{c}, \mathbf{g}$ to P_i .
 - 3 **Party P_i** randomly chooses $\alpha \in \mathbb{Z}_q$, creates \mathbf{y}' , and computes the value a, h . Then, P_i sends only h to P_0
 - 4 **All Parties jointly compute**
 $\langle z \rangle = \langle \beta \rangle - \langle \alpha \rangle = \langle \frac{1}{b} \rangle \cdot \langle a \rangle + \langle \frac{hR_2}{bR_3} \rangle - \langle \alpha \rangle$ using MPC
-

random vectors $\mathbf{x}_i \in \mathbb{R}^{L+1}$, $i \in \{1, \dots, r-1, r+1, \dots, d\}$ to create a matrix $\mathbf{X} \in \mathbb{R}^{d \times (L+1)}$, whose i -th row ($i \neq r$) is \mathbf{x}_i and r -th row is $\mathbf{x}'^T = (x_1, \dots, x_L, 1)$. Then, P_0 locally computes $\mathbf{b} = \sum_{j=1}^d \mathbf{Q}_{j,r}$, $\mathbf{U} = \mathbf{Q} \cdot \mathbf{X}$, $\mathbf{c} = \sum_{i \in \{1, \dots, d\}, i \neq r} (\mathbf{x}_i^T \cdot \sum_{j=1}^d \mathbf{Q}_{j,i}) + R_1 R_2 \mathbf{f}^T$, $\mathbf{g} = R_1 R_3 \mathbf{f}$, and sends $\mathbf{U}, \mathbf{c}, \mathbf{g}$ to P_i ; 2) P_i chooses a random value α to generate $\mathbf{y}' = (y_1, \dots, y_L, \alpha)^T$, computes and sends to P_0 two scalars $a = \sum_{j=1}^d \mathbf{U}_j \cdot \mathbf{y}' - \mathbf{c} \cdot \mathbf{y}'$ and $h = \mathbf{g}^T \cdot \mathbf{y}'$; 3) P_0 locally computes $\beta = \frac{a}{b} + \frac{hR_2}{bR_3}$. The result satisfies $\beta - \alpha = \mathbf{x}^T \cdot \mathbf{y}$. We refer interested readers to [39] for proof of correctness.

The *Euclidean distance computation* in our federated shapelet search can benefit from the above protocol, since each $\|S, T_j^i[p, L_S]\|^2$ can be represented as

$$\|S, T_j^i[p, L_S]\|^2 = \sum_{p'=1}^{L_S} (s_{p'})^2 + \sum_{p'=1}^{L_S} (t_{p'+p-1})^2 + 2 \sum_{p'=1}^{L_S} s_{p'} t_{p'+p-1}, \quad (4)$$

where the term $z = \sum_{p'=1}^{L_S} s_{p'} t_{p'+p-1} = S^T \cdot T_j^i[p, L_S]$ can be computed by P_0 and P_i jointly executing the protocol to get β and α , respectively. The terms $\sum_{p'=1}^{L_S} (s_{p'})^2$ and $\sum_{p'=1}^{L_S} (t_{p'+p-1})^2$ can be locally computed by the two parties. To this end, all parties aggregate the three terms in secret shares using non-interactive secure addition. In this way, the total communication cost for the $(N - L_S + 1)(M - M_0)$ Euclidean distances between S and the sub-series of the participants is reduced from $O(L_S(N - L_S + 1)(M - M_0))$ to $O(L_S) + O((N - L_S + 1)(M - M_0))$.

6.2 Security Analysis and Enhancement

Although the protocol in Algorithm 2 benefits the efficiency of the distance computation, it is unavaliable due to the security issue.

THEOREM 4. *The protocol of Algorithm 2 is insecure under the security defined in Definition 1.*

PROOF SKETCH. Consider an adversary \mathcal{A} that attacks P_0 . By executing the raw protocol in Algorithm 2, \mathcal{A} receives the messages a and h . For ease of exposition, we represent the matrix \mathbf{U} as a row of the column vectors, i.e., $\mathbf{U} = (\mathbf{u}_1, \dots, \mathbf{u}_{L+1})$, and denote $\mathbf{c} = (c_1, \dots, c_{L+1})$ and $\mathbf{g}^T = (g_1, \dots, g_{L+1})$. Recall that $\mathbf{v}' = (\mathbf{v}^T, \alpha)^T$. Thus, it has

$$a = \sum_{j=1}^d \mathbf{U}_j \cdot \mathbf{v}' - \mathbf{c} \cdot \mathbf{v}' = \mathbf{e}_1^T \cdot \mathbf{v} + w\alpha, \quad (5)$$

$$h = \mathbf{g}^T \cdot \mathbf{v}' = \mathbf{e}_2^T \cdot \mathbf{v} + g_{L+1}\alpha, \quad (6)$$

where $\mathbf{e}_1 = (\sum \mathbf{u}_1 + c_1, \dots, \sum \mathbf{u}_L + c_L)^T$, $w = (\sum \mathbf{u}_{L+1} + c_{L+1})$, and $\mathbf{e}_2 = (g_1, \dots, g_L)^T$. Based on Eq 5-6, \mathcal{A} knows that $g_{L+1}a - wh = (g_{L+1}\mathbf{e}_1^T - w\mathbf{e}_2^T) \cdot \mathbf{v}$, where $g_{L+1}\mathbf{e}_1^T - w\mathbf{e}_2^T$ is created locally in P_0 . Obviously, the probability distribution of $g_{L+1}a - wh$ is dependent on the private data \mathbf{v} , which cannot be simulated by any \mathcal{S} . \square

Our novel protocol Π_{DP} . To securely achieve the acceleration, we propose Π_{DP} , a novel dot-product protocol that follows the security in Definition 1. The basic idea is to enhance the security of Algorithm 2 using MPC and the finite field arithmetic. This solution is simple but rather effective in terms of both security and efficiency.

Π_{DP} is presented in Algorithm 3. It has three differences to the raw protocol: i) P_0 and P_i represent each element of their input vectors as fixed-point number encoded in \mathbb{Z}_q as used in MPC [4, 16, 17] (Algorithm 3 Line 1), generates each random masking value from the same field \mathbb{Z}_q , and compute $\mathbf{b}, \mathbf{U}, \mathbf{c}, \mathbf{g}$, and a, h in \mathbb{Z}_q [17] (Algorithm 3 Lines 2-3); ii) P_i only sends h to P_0 but keeps a private (Algorithm 3 Line 3); iii) the value $\beta - \alpha$ is jointly computed by the two parties using MPC (Algorithm 3 Line 4). Note that the protocol incurs only one additional interactive operation when computing $\langle z \rangle = \langle \frac{1}{b} \rangle \langle a \rangle$. Thus, computing the Euclidean norm between S and the $M - M_0$ series requires still $O(L_S) + O((N - L_S + 1)(M - M_0))$, which is *much smaller* compared to the directly using of the MPC operations in $\Pi_{FedSS-B}$.

More importantly, we verify the security guarantee of Π_{DP} .

THEOREM 5. *Π_{DP} is secure under the security definition defined in Definition 1.*

PROOF SKETCH. Since the secretly-sharing-based MPC are secure, we focus on the messages beyond it. We describe two simulators \mathcal{S}_0 and \mathcal{S}_i that simulate the messages of the adversaries for party P_0 and P_i , respectively.

We first present \mathcal{S}_0 . Similar to Eq 6, when receiving the message h , the adversary knows $h = (\mathbf{e}_2^T \cdot \mathbf{v} + g_{L+1}\alpha) \bmod q$. Since the masking values \mathbf{e}_2^T , g_{L+1} , and α are independently and uniformly sampled from \mathbb{Z}_q , the distribution of h is equal to $h' = g_{L+1}\alpha \bmod q$. In the ideal interaction, \mathcal{S}_0 independently and randomly chooses α and g_{L+1} from \mathbb{Z}_q to compute and send h' to the adversary. Indeed the views of the environment in both ideal and real interactions are indistinguishable.

Next, we discuss \mathcal{S}_i . By executing Π_{DP} in the real interaction, the adversary of P_i receives $\mathbf{U}, \mathbf{c}, \mathbf{g}$. Both \mathbf{c} and \mathbf{g} are derived from independent and randomly chosen values. Thus, \mathcal{S}_i can follow the same procedure to compute them. Without loss of generality, we

assume $r = 1$ and $d = 2$. Then, $U = Q \cdot X$ follows

$$\begin{pmatrix} Q_{1,1}x_1 + Q_{1,2}x_{2,1} & \dots & Q_{1,1}x_L + Q_{1,2}x_{2,L} & Q_{1,1} + Q_{1,2}x_{2,L+1} \\ Q_{2,1}x_1 + Q_{2,2}x_{2,1} & \dots & Q_{2,1}x_L + Q_{2,2}x_{2,L} & Q_{2,1} + Q_{2,2}x_{2,L+1} \end{pmatrix}. \quad (7)$$

Note that we omit the modular operations at each entry for ease of exposition. The value of each entry is masked by a unique triplet, e.g., (Q_{11}, Q_{12}, x_{21}) at the entry $(1,1)$. Because the values of these triplets are independently and randomly chosen from \mathbb{Z}_q , the elements of U are independent and identically distributed. Similar to S_0 , S_i can simulate U by computing U' , where $U'_{i,j} = Q_{i,k}x_{i,j} \bmod q$, $\forall k \in \{1, \dots, d\}$, and sends it along with c, g to the adversary. The views of the environment in both ideal and real interaction are identically distributed.

In summary, the simulators achieve the same effect that the adversaries achieve. The security follows. \square

With the security guarantee, we can integrate Π_{DP} into $\Pi_{FedSS-B}$ to accelerate the distance computation. The protocol Π_{DP} can also serve as a building block for other applications.

7 QUALITY MEASUREMENT ACCELERATION

Empirically, evaluating the shapelet quality using IG with the binary strategy (Section 3.1) is the best practice in terms of TSC accuracy. However, computing IG in the FL setting suffers from a severe efficiency issue. The reasons are: i) a large number (M) of thresholds will be evaluated for each candidate; ii) evaluating different thresholds incurs duplicated interactive operations; iii) evaluating one threshold is already inefficient mainly because the required secure division and logarithm operations are expensive (as illustrated in Figure 2); iv) the IG pruning strategies lose their efficacy due to the security issue (Section 5.3).

To consider both accuracy and efficiency, we propose to speed up the quality measurement in $\Pi_{FedSS-B}$ in two aspects.

O1: Accelerating IG computation. To benefit from IG in terms of TSC accuracy, we propose a speed-up method to reduce as many interactive operations as possible in computing IG based on *secure sorting* (Section 7.1), which tackles the problem in reason ii).

O2: Tapping alternative measures. As the problems of i), iii), and iv) are the *inherent deficiencies* of IG that is difficult to avoid, we propose a trade-off method tailored for the FL setting by tapping other measures that are much more secure-computation-efficient than IG, at the cost of acceptable loss of TSC accuracy (Section 7.2).

7.1 Sorting-based IG Acceleration

The straightforward IG computation in Section 5.1 is inefficient since it incurs $O(M^2)$ *secure comparisons* for $\langle y_L \rangle$, and $O(M^2)$ *secure multiplications* for $\langle |DS_{\tau,L,y(S)}| \rangle$ and $\langle |DS_{\tau,R,y(S)}| \rangle$. Inspired by [71] and [3], we propose to securely reduce the duplicated interactive operations by pre-sorting the secretly shared distances and labels before computing each $Q_{IG}(S)$.

Assuming $\langle D_S \rangle = \bigcup_{i=0}^{n-1} \{ \langle d_{T_j^i, S} \rangle \}_{j=1}^{M_i}$ are arranged in an *ordered sequence* $\langle D_S' \rangle = \{ \langle d_j \rangle \}_{j=1}^M$ where $d_{j_1} < d_{j_2}$ for any $1 \leq j_1 < j_2 \leq M$, we can know $y_L' = y_{DS_{\tau,L} \subseteq DS'}$ for each threshold $\langle \tau \rangle = \langle d_j \rangle$ without using secure comparison, where $y_L'[j'] = 1$ for $j' < j$ and 0 otherwise. Meanwhile, if $\langle y_{c_i} \rangle (i \in \{1, \dots, C\})$ is permuted into $\langle y_{c_i'} \rangle$ such that each entry j' for $\langle y_{c_i'} \rangle$ and $\langle d_{T_j^i, S} \rangle$ indicates the same sample, i.e., $\langle y_{c_i'} \rangle[j'] = \langle y_{c_i} \rangle[j]$ when $\langle d_{j'} \rangle$ is

$\langle d_{T_j^i, S} \rangle (j' \in \{1, \dots, M\})$, we can compute the statistics in Eq. 3 by replacing $\langle y_L \rangle$, $\langle y_R \rangle$, and $\langle y_{c_i} \rangle$ with y_L' , $y_R' = 1 - y_L'$, and $\langle y_{c_i'} \rangle$, respectively. Note that the newly produced y_L' is in plaintext thanks to the order of $\langle DS' \rangle$. Thus, it requires only $O(C)$ secure multiplications to compute the statistics in Eq 3 for each threshold, where C is a small constant representing the number of classes.

Based on the above observation, the key to the acceleration is to *securely sort* the secretly shared *distances* and the *indicating vectors* of the class labels. We achieve this goal by using the *secure comparison* and *assignment* (Section 3.2) for a data-independent *sorting network* [9, 12]. The distance vector $\langle D_S \rangle$ is taken as the sorting key to permute both $\langle D_S \rangle$ and $\langle y_{c_i} \rangle (i \in \{1, \dots, C\})$ consistently. The output corresponds to the assumption above. The sorting network takes $O(M \log^2 M)$ interactive operations for the input of size M [9]. Therefore, the complexity of computing each $\langle Q_{IG}(S) \rangle$ becomes $O(M \log^2 M)$, which is much smaller than the $O(M^2)$ in $\Pi_{FedSS-B}$.

THEOREM 6. *The sorting-based acceleration is secure under the security definition defined in Definition 1.*

PROOF SKETCH. The only difference between the acceleration method and the basic protocol for the IG computation is the usage of the secure sorting algorithm, which is proved to be secure [12]. Thus, the security of the sorting-based acceleration follows. \square

7.2 Alternative-measures-based Trade-off

As discussed at the beginning of Section 7, although IG is superior in TSC accuracy, it is naturally difficult to efficiently compute the measure. To further accelerate the shapelet quality assessment step, we propose to tap *alternative measures* that can be securely and more efficiently achieved in the FL setting, while guaranteeing comparable TSC accuracy.

There are other shapelet quality measures, such as Kruskal-Wallis (KW) [55], Mood's Median (MM) [55], and ANOVA F (F-stat) test [37]. However, these measures are less considered in recent works [7, 14, 67], since they have no significant advantage over IG in terms of both accuracy and efficiency, when the binary strategy [14] and the IG pruning technique [71] are integrated. In the brand new FL scenario, the *expensive communication cost* incurred by interactive operations and the *failure of the pruning* for computing IG remind us to reexamine these alternatives.

F-stat-based quality measurement. As shown in [37], using F-stat for TSC is *a little better* than KW and MM in terms of accuracy. More essentially, F-stat performs with $O(M)$ secure multiplications and $C + 1$ secure divisions in the FL setting, while both KW and MM require $O(M \log^2 M)$ secure comparison and multiplication operations because they rely on secure sorting, and they also need C times of divisions. Thus, we choose F-stat as the alternative measure to achieve the trade-off.

Given $D_S = \{d_{T_j, S}\}_{j=1}^M$ and $\{y_j\}_{j=1}^M$ where $y_j \in \{c_i\}_{i=1}^C$, the F-stat is defined as:

$$Q_F(S) = \frac{\sum_{i=1}^C (\bar{D}_{S, c_i} - \bar{D}_S)^2 / (C - 1)}{\sum_{i=1}^C \sum_{y_j = c_i} (d_{T_j, S} - \bar{D}_{S, c_i})^2 / (M - C)}, \quad (8)$$

where $\bar{D}_{S, c_i} = \frac{\sum_{d \in D_{S, c_i}} d}{|D_{S, c_i}|}$ is the mean distance w.r.t. class c_i with $D_{S, c_i} = \{d_{T_j, S} | y_j = c_i\}_{j=1}^M$, and \bar{D}_S is the mean of all distances.

Similar to the IG computing in Section 5.1, we leverage the *indicating vector* to indicate whether each sample belongs to each of the C classes. Given $\langle D_S \rangle = \bigcup_{i=0}^{n-1} \{ \langle d_{T_j^i, S} \rangle \}_{j=1}^{M_i}$ and $\langle y_{c_i'} \rangle =$

$(\langle \mathbf{y}_{TD_{c_{i'}}^0 \subseteq TD^0}^0 \rangle, \dots, \langle \mathbf{y}_{TD_{c_{i'}}^{n-1} \subseteq TD^{n-1}}^{n-1} \rangle)$, the parties jointly compute the terms $\langle \overline{D}_{S, c_{i'}} \rangle = \frac{\langle D_S \rangle \cdot \langle \mathbf{y}_{c_{i'}} \rangle}{\langle \mathbf{y}_{c_{i'}} \rangle \cdot 1}$, $\langle \overline{D}_S \rangle = \frac{\langle D_S \rangle \cdot 1}{M}$, and $\sum_{y_j=c_{i'}} (d_{T_j, S} - \overline{D}_{S, c_{i'}})^2 = \langle d_{c_{i'}} \rangle \cdot \langle d_{c_{i'}} \rangle$ where $\langle d_{c_{i'}} \rangle[j] = \langle \mathbf{y}_{c_{i'}} \rangle[j] \cdot (\langle d_{T_j, S} \rangle - \overline{D}_{S, c_{i'}})$, $j \in \{1, \dots, M\}$. Then, they can jointly compute $\langle Q_F(S) \rangle$.

The protocol for $\langle Q_F(S) \rangle$ has a complexity of $O(M)$, while the computation of $\langle Q_{IG}(S) \rangle$ using our optimization in Section 7.1 still takes $O(M \log^2 M)$. Our empirical evaluation in Section 8.3 shows that the F-stat-based FedST achieves comparable accuracy to the prior IG-based solution.

THEOREM 7. *The F-stat-based shapelet quality measurement is secure under the security definition defined in Definition 1.*

PROOF SKETCH. Similar to the IG-based method in Section 5.1 and Section 7.1, the input and output of the F-stat are both secret shares. The MPC operations and indicating vectors are used to make the computation indistinguishable. The security follows. \square

8 EXPERIMENTS

In this section, we empirically evaluate the effectiveness of the FedST method and the acceleration techniques.

8.1 Experimental Setup

Our experimental setups are as follows:

Implementation. FedST is implemented in Python. We utilize the SPDZ library [42] for semi-honest additive-secret-sharing-based MPC. The security parameter is set to $\kappa = 40$, which ensures that the probability of information leakage, i.e., the quantity in Definition 1 is less than $2^{-\lambda}$ ($\lambda = \kappa$) [16, 17].

Environment. We build a cross-silo federated learning environment by running parties in isolated 16G RAM and 8 core Platinum 8260 CPUs docker containers installed with Ubuntu 20.04 LTS. The parties communicate with each other through the docker bridge network with 4Gbps bandwidth.

Datasets. We use both the *real-world datasets* and the *synthetic datasets* for evaluation at the following two different scales.

- To evaluate the effectiveness of FedST, we use the popular 112 TSC datasets of the UCR Archive [24] that are collected from different types of applications, such as ECG or motion recognition. In the cross-silo and horizontal setting, each business has considerable but insufficient training samples for every class. Thus, we randomly partition the training samples of each class into n equal-size subsets. Since there are 15 small datasets that cannot be partitioned as above, we omit them and conduct experiments on the remaining 97 datasets.

- To investigate the effectiveness of the acceleration techniques, we first assess the efficiency improvement of these techniques using the synthetic datasets. Since the secure computation is data-independent, we randomly generate the synthetic datasets of varying parameters. Next, we compare the F-stat to the prior IG measure in terms of both accuracy and efficiency on the 97 UCR datasets to validate the effectiveness of the trade-off.

Metrics. We use the *accuracy* to evaluate the classification, which is measured as the number of samples that are correctly predicted over the total testing datasets. For efficiency, we measure the *running time* of the protocols in each step.

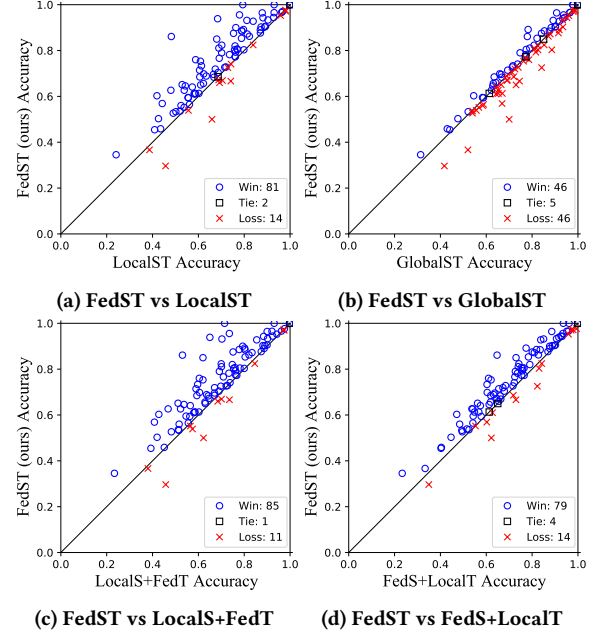


Figure 4: Pairwise comparison between FedST and the baselines on 97 UCR datasets. The blue/black/red scatters represent the datasets where FedST wins/ties/loses the competitors.

8.2 Effectiveness of the FedST framework

Baselines. Since the advantage of the shapelet transformation against other TSC methods has been widely shown [7, 8, 67], we focus on investigating the *effectiveness of enabling FL for TSC* in terms of classification accuracy. To achieve this goal, we compare our FedST with the four baselines:

- LocalST: the traditional TSC solution that P_0 performs the centralized shapelet transformation with only its own data;
- GlobalST: the ideal solution that P_0 uses the data of all parties for centralized shapelet transformation without privacy protection;
- LocalS+FedT: a variant of FedST that P_0 executes the shapelet search step locally and collaborates with the participants for federated data transformation and classifier training;
- FedS+LocalT: a variant of FedST that P_0 locally performs data transformation and classifier training using the shapelets found through federated shapelet search.

To enable a fair comparison, we implement a random forest of 40 trees with the same hyper-parameters as the classifier over the transformed data for all the methods. The candidates are sampled with the length ranging from $\min(3, \frac{N}{4})$ to N . The number of shapelets K is set to 200 and the number of parties n is set to 3. The prior IG is used for assess the shapelet quality.

Pairwise comparison. Figure 4 reports the pairwise accuracy comparison of our FedST against the competitors.

Figure 4a shows that FedST is more accurate than the LocalST on most of the datasets. It indicates the effectiveness of our basic idea of enabling FL to improve the TSC accuracy. Figure 4b shows that FedST achieves accuracy close to the non-private GlobalST, which coincides with our analysis in Section 5.2. The slight difference can be caused by two reasons. First, the global method samples the shapelets from all parties, while in FedST the candidates are only generated by P_0 for the interpretability constraints. Second, in secret

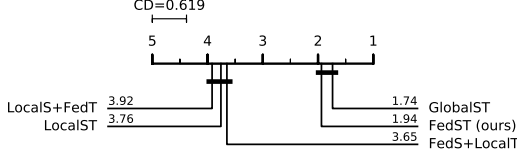


Figure 5: Critical difference diagram for our FedST and the baselines under the statistical level of 0.05.

sharing, the float values are encoded in fixed-point representation for efficiency, which results in the truncation. Fortunately, we show later in Figure 5 that there is no statistically significant difference in accuracy between FedST and GlobalST. From Figure 4c and Figure 4d, we can see that both the variants are much worse than FedST. It means that both the stages of FedST are indispensable.

Multiple comparisons. We present the critical difference diagram [27] of the methods in Figure 5. It reports the *mean ranking of accuracy* among the 97 UCR datasets. The competitors falling in one clique (the bold horizontal line) have no statistically significant difference, while the opposite for the methods from different cliques. Figure 5 shows that FedST is slightly worse than GlobalST and significantly outperforms LocalST. It is notable that the variant conducting only local shapelet search (LocalS+FedT), even with more transformed data, is slightly inferior to LocalST. The reason could be that the locally selected shapelets have poor quality due to the lack of training data, which may cause the transformed data to be more misleading to degrade the accuracy. In comparison, FedS+LocalT performs better than LocalST, because the shapelet quality is improved by FL with more training data used for shapelet search. The two variants are much inferior to our FedST, which indicates the importance of FL for both stages.

8.3 Effectiveness of the acceleration techniques

Efficiency improvement. To assess the effectiveness of the proposed acceleration techniques, we first investigate their *efficiency improvement* using the synthetic datasets of varying dataset size (M), time series length (N), number of parties (n) and candidate set size $|SC|$. The average length of the shapelet candidates is set as $0.6N$ and the number of shapelets K is set as 200. Overall, the results presented in Figure 6 coincide with our complexity analysis.

1) Distance computation. Figure 6a-6c report the time of computing the shapelet distance between a candidate S and all training samples T_j^i ($i \neq 0$) w.r.t. M , N , and n . The time for both $\Pi_{FedSS-B}$ that directly uses MPC (d -MPC) and the optimization leveraging the proposed secure dot-product protocol (d -MPC+ Π_{DP}) scale linearly to M and n . However, d -MPC+ Π_{DP} can achieve up to 30x of speedup over d -MPC for the default $N = 100$. The time of d -MPC increases more quickly than d -MPC+ Π_{DP} as N increases, because the complexity of d -MPC is quadratic w.r.t. N while our proposed d -MPC+ Π_{DP} has a linear complexity of interactive operations.

We also show the time of finding the minimum Euclidean distance (Find-Min), which is a subroutine of the shapelet distance computation. The results show that Find-Min is much faster than d -MPC, which is consistent with our analysis in Section 6 that the time of d -MPC is dominated by the *Euclidean distance computation*. In comparison, the time of d -MPC+ Π_{DP} is very close to the time of Find-Min because the Euclidean distance computation time is substantially reduced (more than 58x speedup) with our Π_{DP} .

2) Quality measurement. We show the time of quality measurement for each candidate S with varying M and n in Figure 6d-6e. Compared to the basic protocol of computing IG in $\Pi_{FedSS-B}$ (Q_{IG}), our proposed secure-sorting-based computation (Q_{IG} +Sorting) achieves a similar performance when M is small, but the time of Q_{IG} increases much faster than Q_{IG} +Sorting as M increases because Q_{IG} has a quadratic complexity to M . In comparison, the time of Q_{IG} +Sorting is dominated by the secure sorting protocol (Sorting), which has a complexity of $O(M \log^2 M)$. The optimized Q_{IG} +Sorting is also more scalable to n than Q_{IG} .

Using F-stat in the quality measurement step (Q_F) can achieve more than 65x of speedup over the optimized Q_{IG} +Sorting. It is also noteworthy that Q_F is much faster than Sorting which bottlenecks the time of securely computing the KW and MM, as mentioned in Section 7.2. That is why we consider the F-stat for the acceleration.

3) Federated shapelet search. Finally, we assess the *total running time of the federated shapelet search protocol* with each proposed acceleration technique. The results are reported in Figure 6f-6i.

Overall, an individual Π_{DP} -based acceleration (+ Π_{DP}) brings 1.01-73.59x of improvement over $\Pi_{FedSS-B}$. The sorting-based (+Sorting) technique gives 1.01-96.17x of speedup alone and the F-stat-based method (+ Q_F) individually achieves 1.01-107.76x of speedup. The combination of these techniques is always more effective than each individual. Π_{DP} -based and Sorting-based methods together (+ Π_{DP} +Sorting) contribute 15.12-630.97x of improvement, while the combination of the Π_{DP} -based and F-stat-based techniques (+ Π_{DP} + Q_F) boosts the protocol efficiency by 32.22-2141.64x.

We notice from Figure 6f that the time of $\Pi_{FedSS-B}$ is dominated by the distance computation when M is small. In this case, + Π_{DP} is more effective. With the increase of M , the quality measurement step gradually dominates the efficiency. As a result, the +Sorting and + Q_F play a more important role in acceleration. Similarly, Figure 6g shows that the efficiency is dominated by the quality measurement when N is small and is gradually dominated by the distance computation with N increases. The acceleration techniques for these two steps are always complementary with each other.

It is also worth noting that the time of all competitors is nearly *in direct proportion to $|SC|$* , as shown in Figure 6i. The result is consistent with our analysis in Section 5.2 that the time for securely *finding the top-K candidates* (Algorithm 1 Line 10), which has a complexity of $O(K \cdot |SC|)$, is *negligible* compared to the time of distance computation and quality measurement. That is why we mainly dedicate to accelerating these two steps.

Effectiveness of the trade-off strategy. We investigate the effectiveness of the F-stat-based protocol in *trading off TSC accuracy and the protocol efficiency*. Specifically, we evaluate both the accuracy and the federated shapelet search time for the two versions of FedST that adopt either the prior Q_{IG} (FedST- Q_{IG}) or the more efficient Q_F (FedST- Q_F). The experiments are conducted using 97 UCR datasets with the same setting as Section 8.2. Both the Π_{DP} -based and the sorting-based speedup methods are adopted.

As shown in Figure 7 top, FedST- Q_F is faster than FedST- Q_{IG} on all 97 datasets. The efficiency improvement is 1.04-8.31x while the average speedup on the 97 datasets is 1.79x. Meanwhile, FedST- Q_F is better than FedST- Q_{IG} on 41 of the 97 datasets in terms of accuracy (Figure 7 bottom). The average accuracy of FedST- Q_F is just 0.5% lower than that of FedST- Q_{IG} . Figure 8 shows the critical difference diagram for these two methods and the two FL baselines (LocalST and GlobalST). The result indicates that FedST- Q_F achieves the same level of accuracy as FedST- Q_{IG} and GlobalST,

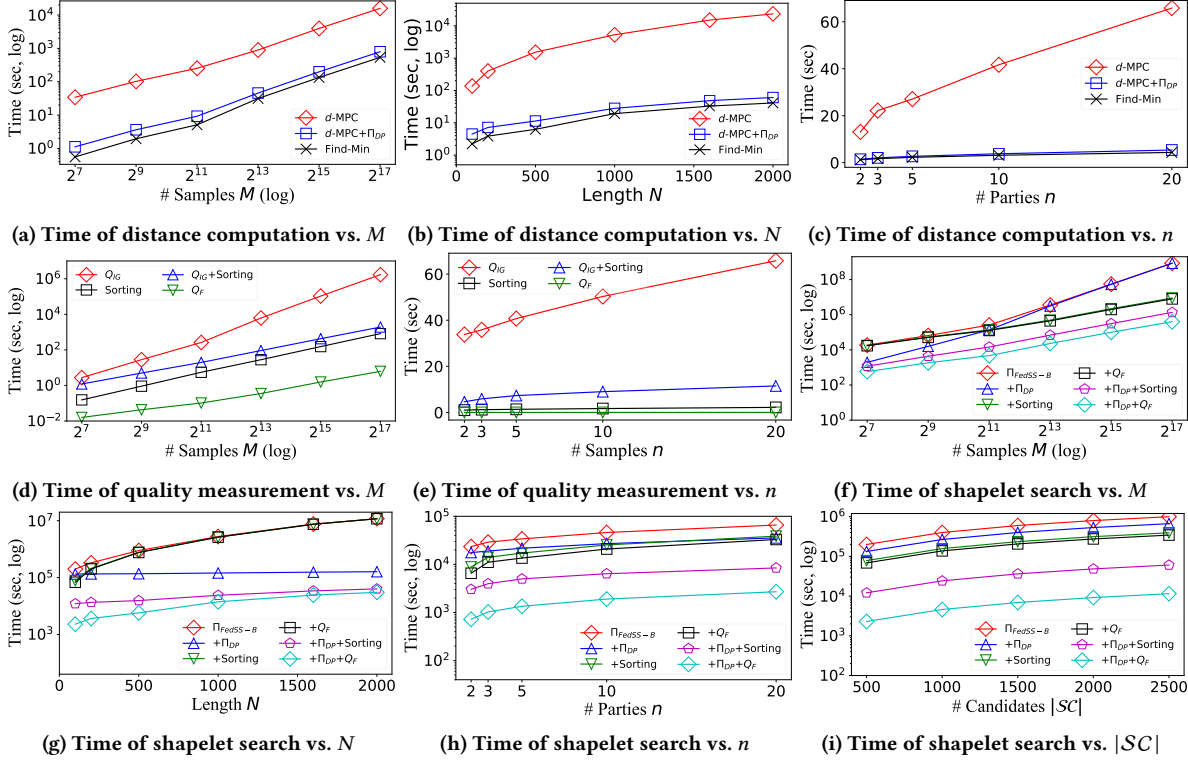


Figure 6: Performance of varying dataset size M (default 512), series length N (default 100), number of parties n (default 3), and candidate set size $|SC|$ (default 500).

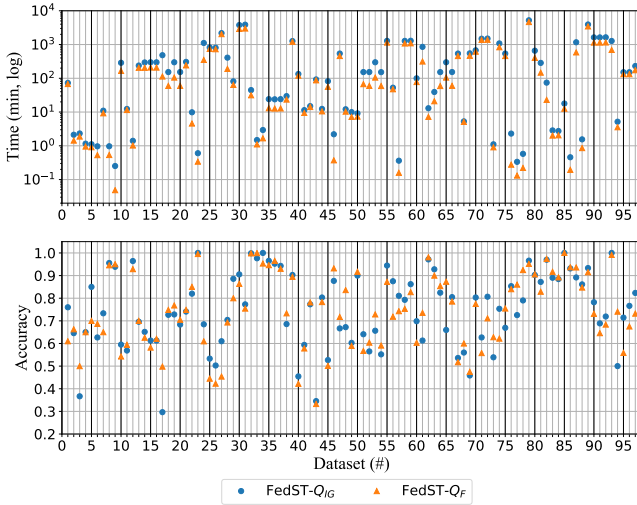


Figure 7: Accuracy and federated shapelet search time of FedST using different quality measures.

and is significantly better than LocalST. In summary, our proposed F-stat-based trade-off strategy can effectively improve the efficiency of the federated shapelet search while guaranteeing comparable accuracy to the superior IG-based method.

8.4 Study of Interpretability

Figure 9 demonstrates the interpretability of FedST using a real-world motion classification problem. The data track the centroid

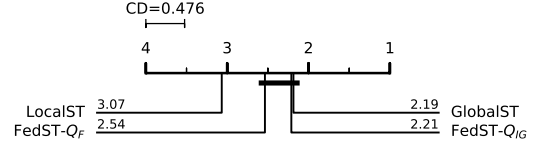


Figure 8: Critical difference diagram for FedST that uses different quality measures and the two baselines. The statistical level is 0.05.

of the actors' right hand for two types of motions. For 'Gun' class, they draw a replicate gun from a hip-mounted holster, point it at a target, then return the gun to the holster and their hands to their sides. For 'No gun (Point)', the actors have their gun by their sides, point with their index fingers to a target, and then return their hands. The best shapelets of the two classes are shown in Figure 9a, which represents the class-specific features, i.e., the hand tracks of drawing the gun (S_1) and putting down the hand (S_2). We transform all time series samples into the distances to these two shapelets and visualize the results in Figure 9b. As can be seen, the time series of class 'Gun' (red) is more similar to S_1 and more distant from S_2 , and the opposite for the 'No gun' data (blue), which explains how FedST makes prediction based on the shapelets.

8.5 Study of Flexibility

We further investigate the flexibility of FedST as discussed in Section 4.1. We evaluate the accuracy and real running time on each of the 97 UCR datasets with the time contract varying from 10% to 90% of the maximum running time (the running time evaluated

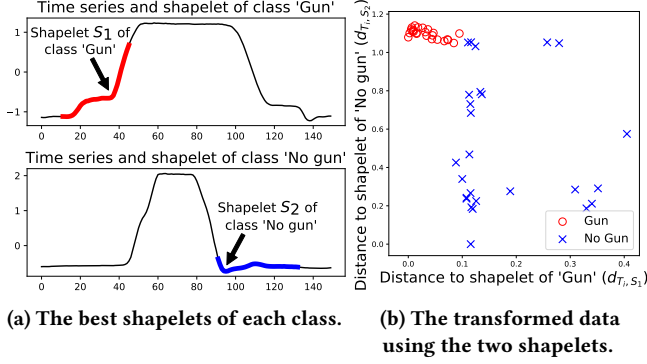


Figure 9: Interpretation of FedST on GunPoint.

in Section 8.2). Figure 10 reports the results. Overall, the accuracy increases with more time is allowed, while the real running time is always close to the contract. It validates the effectiveness of trading off the accuracy and efficiency using the user-defined time contract, which is beneficial for the practical utility.

9 RELATED WORK

Our work is related to federated learning, interpretable time series classification, and privacy preservation.

Federated Learning. Recently, there have been numerous works that dedicate to the federated learning of the general models, including the linear models [5, 18, 69, 73, 92], the tree models [3, 21, 30, 31, 50, 89], and the neural networks [1, 13, 32, 62–64, 79, 95]. However, none of them achieve the same goal as our solution, because these general models are either inaccurate (for the linear and tree models) or hard to interpret (for the neural networks) in tackling the TSC problem [8]. There are also FL solutions designed for specific tasks [19, 38, 52, 53, 58, 59, 64, 72, 80, 85, 87]. These methods target scenarios that are completely different from ours. As a result, we propose to tailor FL method for interpretable TSC. We contribute to proposing the secure, interpretable, and accurate FedST framework, and designing the specific techniques to adapt the federated shapelet search and tackle the efficiency bottlenecks, while any secure federated classifier training solution that complements our solution [3, 20, 69, 97] can be seamlessly integrated.

Interpretable Time Series Classification. While many works dedicate to proposing techniques to better explain the models or instances [6, 22, 84], they are orthogonal to our work since we aim to satisfy the requirements under the FL setting to ensure the TSC models interpretable to the initiator (Section 2.1).

In summary, there are four types of TSC methods based on explainable features, i.e., the distance-based methods [2] that perform prediction and interpretation using the 1-NN instance, the shapelet-based methods [14, 36, 37, 48, 54, 71, 94] that determine the class based on the localized shapes, the interval-based methods [15, 65, 67] that classify the time series based on the statistics at some intervals, and the dictionary-based approaches [46, 47, 66, 68] that utilize the pattern frequency as features. These types of methods can be complement with each other to contribute to higher accuracy [7, 56, 67]. However, the distance-based methods cannot be adapted to our FL setting because they must reveal the 1-NN series to the initiator for explanation while it can violate the data privacy. As for the other types of methods, our work focuses on

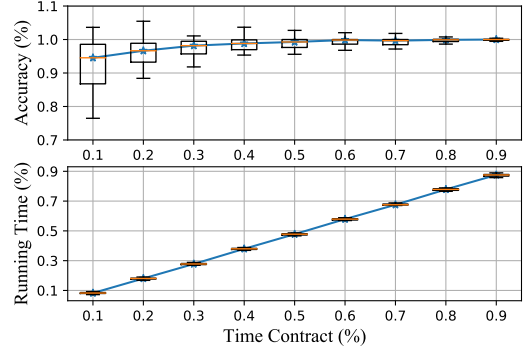


Figure 10: The accuracy (top) and real running time (bottom) w.r.t. the user-defined time contract.

developing a novel framework with a series of optimization techniques based on the shapelet-based approaches, while we would like to leave the works of enabling interval-based and dictionary-based methods for federated TSC in the future.

Privacy Preservation. Data privacy is one of the most essential problems in FL [41, 51, 91]. Several techniques have been studied by existing works. Secure Multi-Party Computation [93] is a general framework that offers secure protocols for many arithmetic operations [23, 42, 43]. These operations are efficient for practical utility [4, 20, 50, 52, 69, 89] under the semi-honest model that most FL works consider, while they can also be extended to the malicious model through zero-knowledge proofs [34]. Homomorphic Encryption (HE) is also a popular technique in FL [21, 31, 59, 89, 95], which allows a simple implementation of the secure addition. However, HE does not support some complex operations (e.g., division and comparison). The encryption and decryption are also computationally intensive [31, 89]. An orthogonal line of works adopt the Differential Privacy (DP) for privacy protection by adding noises to the private data [53, 57, 74, 87, 88]. These methods can be complement with the MPC-based and HE-based FL solutions.

10 CONCLUSION AND FUTURE WORKS

This work studies how to enable FL for interpretable TSC. We are the first to study on this essential topic. We formulate the problem and identify the interpretability constraints under the FL setting. We systematically investigate existing TSC solutions for the centralized scenario and propose FedST, a novel FL-enabled TSC framework based on the centralized shapelet transformation. We design the security protocol FedSS-B for the FedST kernel, analyze its effectiveness, and identify its efficiency bottlenecks. To accelerate the protocol, we propose specific optimizations tailored for the FL setting. Both theoretical analysis and experiment results show the effectiveness of our proposed FedST framework and the acceleration techniques.

In the future, we would like to dedicate to orthogonal works that tackle the FL-enabled TSC problem based on other types of interpretable features to complement FedST. Further, we wish to develop high-performance and easy-to-use systems based on our solution to support industrial applications.

ACKNOWLEDGMENTS

This paper was supported by NSFC grant (U1866602).

REFERENCES

- [1] Martin Abadi, Andy Chu, Ian Goodfellow, H Brendan McMahan, Ilya Mironov, Kunal Talwar, and Li Zhang. 2016. Deep learning with differential privacy. In *Proceedings of the 2016 ACM SIGSAC conference on computer and communications security*. 308–318.
- [2] Amaia Abanda, Usue Mori, and Jose A Lozano. 2019. A review on distance based time series classification. *Data Mining and Knowledge Discovery* 33, 2 (2019), 378–412.
- [3] Mark Abspoel, Daniel Escudero, and Nikolaj Volgushev. 2020. Secure training of decision trees with continuous attributes. *Cryptology ePrint Archive* (2020).
- [4] Abdelrahman Aly and Nigel P Smart. 2019. Benchmarking privacy preserving scientific operations. In *International Conference on Applied Cryptography and Network Security*. Springer, 509–529.
- [5] Yoshinori Aono, Takuya Hayashi, Le Trieu Phong, and Lihua Wang. 2016. Scalable and secure logistic regression via homomorphic encryption. In *Proceedings of the Sixth ACM Conference on Data and Application Security and Privacy*. 142–144.
- [6] Alejandro Barredo Arrieta, Natalia Díaz-Rodríguez, Javier Del Ser, Adrien Bernet, Siham Tabik, Alberto Barbado, Salvador García, Sergio Gil-López, Daniel Molina, Richard Benjamins, et al. 2020. Explainable Artificial Intelligence (XAI): Concepts, taxonomies, opportunities and challenges toward responsible AI. *Information fusion* 58 (2020), 82–115.
- [7] Anthony Bagnall, Michael Flynn, James Large, Jason Lines, and Matthew Middlehurst. 2020. A tale of two toolkits, report the third: on the usage and performance of HIVE-COTE v1. 0. *arXiv e-prints* (2020), arXiv–2004.
- [8] A. Bagnall, J. Lines, A. Bostrom, J. Large, and E. Keogh. 2017. The Great Time Series Classification Bake Off: a Review and Experimental Evaluation of Recent Algorithmic Advances. *Data Mining and Knowledge Discovery* 31 (2017), 606–660. Issue 3.
- [9] Kenneth E Batcher. 1968. Sorting networks and their applications. In *Proceedings of the April 30–May 2, 1968, spring joint computer conference*. 307–314.
- [10] Donald Beaver. 1991. Efficient multiparty protocols using circuit randomization. In *Annual International Cryptology Conference*. Springer, 420–432.
- [11] Donald J Berndt and James Clifford. 1994. Using dynamic time warping to find patterns in time series.. In *KDD workshop*, Vol. 10. Seattle, WA, 359–370.
- [12] Dan Bogdanov, Sven Laur, and Riivo Talviste. 2014. A practical analysis of oblivious sorting algorithms for secure multi-party computation. In *Nordic Conference on Secure IT Systems*. Springer, 59–74.
- [13] Keith Bonawitz, Vladimir Ivanov, Ben Kreuter, Antonio Marcedone, H Brendan McMahan, Sarvar Patel, Daniel Ramage, Aaron Segal, and Karn Seth. 2017. Practical secure aggregation for privacy-preserving machine learning. In *proceedings of the 2017 ACM SIGSAC Conference on Computer and Communications Security*. 1175–1191.
- [14] Aaron Bostrom and Anthony Bagnall. 2017. Binary shapelet transform for multiclass time series classification. In *Transactions on Large-Scale Data-and Knowledge-Centered Systems XXXII*. Springer, 24–46.
- [15] Nestor Cabello, Elham Naghizade, Jianzhong Qi, and Lars Kulik. 2020. Fast and accurate time series classification through supervised interval search. In *2020 IEEE International Conference on Data Mining (ICDM)*. IEEE, 948–953.
- [16] Octavian Catrina and Sebastiaan de Hoogh. 2010. Improved primitives for secure multiparty integer computation. In *International Conference on Security and Cryptography for Networks*. Springer, 182–199.
- [17] Octavian Catrina and Amitabh Saxena. 2010. Secure computation with fixed-point numbers. In *International Conference on Financial Cryptography and Data Security*. Springer, 35–50.
- [18] Kamalika Chaudhuri and Claire Monteleoni. 2008. Privacy-preserving logistic regression. *Advances in neural information processing systems* 21 (2008).
- [19] Jiayi Chen and Aidong Zhang. 2022. FedMSplit: Correlation-Adaptive Federated Multi-Task Learning across Multimodal Split Networks. In *Proceedings of the 28th ACM SIGKDD Conference on Knowledge Discovery and Data Mining*. 87–96.
- [20] Valerie Chen, Valerio Pastro, and Mariana Raykova. 2019. Secure computation for machine learning with SPDZ. *arXiv preprint arXiv:1901.00329* (2019).
- [21] Kewei Cheng, Tao Fan, Yilun Jin, Yang Liu, Tianjian Chen, Dimitrios Papadopoulos, and Qiang Yang. 2021. Secureboost: A lossless federated learning framework. *IEEE Intelligent Systems* 36, 6 (2021), 87–98.
- [22] Roberto Confalonieri, Ludovik Coda, Benedikt Wagner, and Tarek R Besold. 2021. A historical perspective of explainable Artificial Intelligence. *Wiley Interdisciplinary Reviews: Data Mining and Knowledge Discovery* 11, 1 (2021), e1391.
- [23] Ivan Damgård, Valerio Pastro, Nigel Smart, and Sarah Zakarias. 2012. Multiparty computation from somewhat homomorphic encryption. In *Annual Cryptology Conference*. Springer, 643–662.
- [24] Hoang Anh Dau, Anthony J. Bagnall, Kaveh Kamgar, Chin-Chia Michael Yeh, Yan Zhu, Shaghayegh Gharghabi, Chotirat Ann Ratanamahatana, and Eamonn J. Keogh. 2018. The UCR Time Series Archive. *CoRR* abs/1810.07758 (2018). arXiv:1810.07758 <http://arxiv.org/abs/1810.07758>
- [25] Oguz Demirci, Vincent P Clark, Vincent A Magnotta, Nancy C Andreasen, John Lauriello, Kent A Kiehl, Godfrey D Pearlson, and Vince D Calhoun. 2008. A review of challenges in the use of fMRI for disease classification/characterization and a projection pursuit application from a multi-site fMRI schizophrenia study. *Brain imaging and behavior* 2, 3 (2008), 207–226.
- [26] Angus Dempster, Daniel F Schmidt, and Geoffrey I Webb. 2021. Minirocket: A very fast (almost) deterministic transform for time series classification. In *Proceedings of the 27th ACM SIGKDD conference on knowledge discovery & data mining*. 248–257.
- [27] Janez Demšar. 2006. Statistical comparisons of classifiers over multiple data sets. *The Journal of Machine learning research* 7 (2006), 1–30.
- [28] S Dheepadharshani, S Anandh, KB Bhavinaya, and R Lavanya. 2019. Multivariate time-series classification for automated fault detection in satellite power systems. In *2019 International Conference on Communication and Signal Processing (ICCSPP)*. IEEE, 0814–0817.
- [29] Finale Doshi-Velez and Been Kim. 2017. Towards a rigorous science of interpretable machine learning. *arXiv preprint arXiv:1702.08608* (2017).
- [30] Wenjing Fang, Derun Zhao, Jin Tan, Chaochao Chen, Chaofan Yu, Li Wang, Lei Wang, Jun Zhou, and Benyu Zhang. 2021. Large-scale secure XGB for vertical federated learning. In *Proceedings of the 30th ACM International Conference on Information & Knowledge Management*. 443–452.
- [31] Fangcheng Fu, Yingxia Shao, Lele Yu, Jiawei Jiang, Huanran Xue, Yangyu Tao, and Bin Cui. 2021. VF2Boost: Very Fast Vertical Federated Gradient Boosting for Cross-Enterprise Learning. In *Proceedings of the 2021 International Conference on Management of Data*. 563–576.
- [32] Fangcheng Fu, Huanran Xue, Yong Cheng, Yangyu Tao, and Bin Cui. 2022. BlindFL: Vertical Federated Machine Learning without Peeking into Your Data. In *Proceedings of the 2022 International Conference on Management of Data*. 1316–1330.
- [33] Mohamed F Ghalwash, Vladan Radosavljevic, and Zoran Obradovic. 2013. Extraction of interpretable multivariate patterns for early diagnostics. In *2013 IEEE 13th International Conference on Data Mining*. IEEE, 201–210.
- [34] Oded Goldreich and Yair Oren. 1994. Definitions and properties of zero-knowledge proof systems. *Journal of Cryptology* 7, 1 (1994), 1–32.
- [35] Daniel Gordon, Danny Hendler, and Lior Rokach. 2012. Fast randomized model generation for shapelet-based time series classification. *arXiv preprint arXiv:1209.5038* (2012).
- [36] Josif Grabocka, Nicolas Schilling, Martin Wistuba, and Lars Schmidt-Thieme. 2014. Learning time-series shapelets. In *Proceedings of the 20th ACM SIGKDD international conference on Knowledge discovery and data mining*. ACM, 392–401.
- [37] Jon Hills, Jason Lines, Edgaras Baranauskas, James Mapp, and Anthony Bagnall. 2014. Classification of time series by shapelet transformation. *Data mining and knowledge discovery* 28, 4 (2014), 851–881.
- [38] Yutao Huang, Lingyang Chu, Zirui Zhou, Lanjun Wang, Jiangchuan Liu, Jian Pei, and Yong Zhang. 2021. Personalized Cross-Silo Federated Learning on Non-IID Data.. In *AAAI* 7865–7873.
- [39] Ioannis Ioannidis, Ananth Grama, and Mikhail Atallah. 2002. A secure protocol for computing dot-products in clustered and distributed environments. In *Proceedings International Conference on Parallel Processing*. IEEE, 379–384.
- [40] Hassan Ismail Fawaz, Germain Forestier, Jonathan Weber, Lhassane Idoumghar, and Pierre-Alain Muller. 2019. Deep learning for time series classification: a review. *Data mining and knowledge discovery* 33, 4 (2019), 917–963.
- [41] Peter Kairouz, H Brendan McMahan, Brendan Avent, Aurélien Bellet, Mehdi Bennis, Arjun Nitin Bhagoji, Kallista Bonawitz, Zachary Charles, Graham Cormode, Rachel Cummings, et al. 2021. Advances and open problems in federated learning. *Foundations and Trends® in Machine Learning* 14, 1–2 (2021), 1–210.
- [42] Marcel Keller. 2020. MP-SPDZ: A versatile framework for multi-party computation. In *Proceedings of the 2020 ACM SIGSAC conference on computer and communications security*. 1575–1590.
- [43] Marcel Keller, Peter Scholl, and Nigel P Smart. 2013. An architecture for practical actively secure MPC with dishonest majority. In *Proceedings of the 2013 ACM SIGSAC conference on Computer & communications security*. 549–560.
- [44] Eamonn Keogh and Shruti Kasetty. 2003. On the need for time series data mining benchmarks: a survey and empirical demonstration. *Data Mining and knowledge discovery* 7, 4 (2003), 349–371.
- [45] Eamonn Keogh, Li Wei, Xiaopeng Xi, Sang-Hee Lee, and Michail Vlachos. 2006. LB_Keogh supports exact indexing of shapes under rotation invariance with arbitrary representations and distance measures. In *Proceedings of the 32nd international conference on Very large data bases*. Citeseer, 882–893.
- [46] James Large, Anthony Bagnall, Simon Malinowski, and Romain Tavenard. 2019. On time series classification with dictionary-based classifiers. *Intelligent Data Analysis* 23, 5 (2019), 1073–1089.
- [47] Thach Le Nguyen, Severin Gsponer, and Georgiana Ifrim. 2017. Time series classification by sequence learning in all-subsequence space. In *2017 IEEE 33rd international conference on data engineering (ICDE)*. IEEE, 947–958.
- [48] Guozhong Li, Byron Choi, Jianliang Xu, Sourav S Bhowmick, Kwok-Pan Chun, and Grace Lai-Hung Wong. 2021. Shapenet: A shapelet-neural network approach for multivariate time series classification. In *Proceedings of the AAAI Conference on Artificial Intelligence*, Vol. 35. 8375–8383.
- [49] Li Li, Yuxi Fan, Mike Tse, and Kuo-Yi Lin. 2020. A review of applications in federated learning. *Computers & Industrial Engineering* 149 (2020), 106854.
- [50] Qibin Li, Zeyi Wen, and Bingsheng He. 2020. Practical federated gradient boosting decision trees. In *Proceedings of the AAAI conference on artificial intelligence*, Vol. 34. 4642–4649.
- [51] Tian Li, Anit Kumar Sahu, Ameet Talwalkar, and Virginia Smith. 2020. Federated learning: Challenges, methods, and future directions. *IEEE Signal Processing Magazine* 37, 3 (2020), 50–60.

- [52] Xiling Li, Rafael Dowsley, and Martine De Cock. 2021. Privacy-preserving feature selection with secure multiparty computation. In *International Conference on Machine Learning*. PMLR, 6326–6336.
- [53] Zitao Li, Bolin Ding, Ce Zhang, Ninghui Li, and Jingren Zhou. 2021. Federated matrix factorization with privacy guarantee. *Proceedings of the VLDB Endowment* 15, 4 (2021), 900–913.
- [54] Zhiyu Liang and Hongzhi Wang. 2021. Efficient class-specific shapelets learning for interpretable time series classification. *Information Sciences* 570 (2021), 428–450.
- [55] Jason Lines and Anthony Bagnall. 2012. Alternative quality measures for time series shapelets. In *International Conference on Intelligent Data Engineering and Automated Learning*. Springer, 475–483.
- [56] Jason Lines, Sarah Taylor, and Anthony Bagnall. 2018. Time series classification with HIVE-COTE: The hierarchical vote collective of transformation-based ensembles. *ACM Transactions on Knowledge Discovery from Data* 12, 5 (2018).
- [57] Junxu Liu, Jian Lou, Li Xiong, Jinfei Liu, and Xiaofeng Meng. 2021. Projected federated averaging with heterogeneous differential privacy. *Proceedings of the VLDB Endowment* 15, 4 (2021), 828–840.
- [58] Yang Liu, Yan Kang, Chaoping Xing, Tianjian Chen, and Qiang Yang. 2020. A secure federated transfer learning framework. *IEEE Intelligent Systems* 35, 4 (2020), 70–82.
- [59] Yejiu Liu, Weiyuan Wu, Lampros Flokas, Jiannan Wang, and Eugene Wu. 2021. Enabling SQL-Based Training Data Debugging for Federated Learning. *Proc. VLDB Endow.* 15, 3 (nov 2021), 388–400. <https://doi.org/10.14778/3494124.3494125>
- [60] Priyanka Mary Mammen. 2021. Federated learning: opportunities and challenges. *arXiv preprint arXiv:2101.05428* (2021).
- [61] Othmane Marfoq, Chuan Xu, Giovanni Neglia, and Richard Vidal. 2020. Throughput-optimal topology design for cross-silo federated learning. *Advances in Neural Information Processing Systems* 33 (2020), 19478–19487.
- [62] Brendan McMahan, Eider Moore, Daniel Ramage, Seth Hampson, and Blaise Agüera y Arcas. 2017. Communication-efficient learning of deep networks from decentralized data. In *Artificial intelligence and statistics*. PMLR, 1273–1282.
- [63] H Brendan McMahan, Eider Moore, Daniel Ramage, and Blaise Agüera y Arcas. 2016. Federated learning of deep networks using model averaging. *arXiv preprint arXiv:1602.05629* 2 (2016).
- [64] H Brendan McMahan, Daniel Ramage, Kunal Talwar, and Li Zhang. 2017. Learning differentially private recurrent language models. *arXiv preprint arXiv:1710.06963* (2017).
- [65] Matthew Middlehurst, James Large, and Anthony Bagnall. 2020. The canonical interval forest (CIF) classifier for time series classification. In *2020 IEEE international conference on big data (big data)*. IEEE, 188–195.
- [66] Matthew Middlehurst, James Large, Gavin Cawley, and Anthony Bagnall. 2020. The temporal dictionary ensemble (TDE) classifier for time series classification. In *Joint European Conference on Machine Learning and Knowledge Discovery in Databases*. Springer, 660–676.
- [67] Matthew Middlehurst, James Large, Michael Flynn, Jason Lines, Aaron Bostrom, and Anthony Bagnall. 2021. HIVE-COTE 2.0: a new meta ensemble for time series classification. *Machine Learning* 110, 11 (2021), 3211–3243.
- [68] Matthew Middlehurst, William Vickers, and Anthony Bagnall. 2019. Scalable dictionary classifiers for time series classification. In *International Conference on Intelligent Data Engineering and Automated Learning*. Springer, 11–19.
- [69] Payman Mohassel and Yupeng Zhang. 2017. Secureml: A system for scalable privacy-preserving machine learning. In *2017 IEEE symposium on security and privacy (SP)*. IEEE, 19–38.
- [70] Christoph Molnar. 2022. *Interpretable Machine Learning* (2 ed.). christophm.github.io/interpretable-ml-book/
- [71] Abdullah Mueen, Eamonn Keogh, and Neal Young. 2011. Logical-shapelets: an expressive primitive for time series classification. In *Proceedings of the 17th ACM SIGKDD international conference on Knowledge discovery and data mining*. 1154–1162.
- [72] Khalil Muhammad, Qinqin Wang, Diarmuid O'Reilly-Morgan, Elias Tragou, Barry Smyth, Neil Hurley, James Geraci, and Aonghus Lawlor. 2020. Fedfast: Going beyond average for faster training of federated recommender systems. In *Proceedings of the 26th ACM SIGKDD International Conference on Knowledge Discovery & Data Mining*. 1234–1242.
- [73] Valeria Nikolaenko, Udi Weinsberg, Stratis Ioannidis, Marc Joye, Dan Boneh, and Nina Taft. 2013. Privacy-preserving ridge regression on hundreds of millions of records. In *2013 IEEE symposium on security and privacy*. IEEE, 334–348.
- [74] Qiying Pan and Yifei Zhu. 2022. FedWalk: Communication Efficient Federated Unsupervised Node Embedding with Differential Privacy. *Proceedings of the 28th ACM SIGKDD Conference on Knowledge Discovery and Data Mining* (2022).
- [75] Claudia Pérez-D'Arpino and Julie A Shah. 2015. Fast target prediction of human reaching motion for cooperative human-robot manipulation tasks using time series classification. In *2015 IEEE international conference on robotics and automation (ICRA)*. IEEE, 6175–6182.
- [76] Thanawin Rakthanmanon, Bilson Campana, Abdullah Mueen, Gustavo Batista, Brandon Westover, Qiang Zhu, Jesin Zakaria, and Eamonn Keogh. 2012. Searching and mining trillions of time series subsequences under dynamic time warping. In *Proceedings of the 18th ACM SIGKDD international conference on Knowledge discovery and data mining*. 262–270.
- [77] Erica Ramirez, Markus Wimmer, and Martin Atzmueller. 2019. A computational framework for interpretable anomaly detection and classification of multivariate time series with application to human gait data analysis. In *Artificial Intelligence in Medicine: Knowledge Representation and Transparent and Explainable Systems*. Springer, 132–147.
- [78] Alejandro Pasos Ruiz, Michael Flynn, James Large, Matthew Middlehurst, and Anthony Bagnall. 2021. The great multivariate time series classification bake off: a review and experimental evaluation of recent algorithmic advances. *Data Mining and Knowledge Discovery* 35, 2 (2021), 401–449.
- [79] Reza Shokri and Vitaly Shmatikov. 2015. Privacy-preserving deep learning. In *Proceedings of the 22nd ACM SIGSAC conference on computer and communications security*. 1310–1321.
- [80] Virginia Smith, Chao-Kai Chiang, Maziar Sanjabi, and Ameet S Talwalkar. 2017. Federated multi-task learning. *Advances in neural information processing systems* 30 (2017).
- [81] Gian Antonio Susto, Angelo Cenedese, and Matteo Terzi. 2018. Time-series classification methods: Review and applications to power systems data. *Big data application in power systems* (2018), 179–220.
- [82] Chang Wei Tan, Angus Dempster, Christoph Bergmeir, and Geoffrey I Webb. 2022. MultiRocket: Multiple pooling operators and transformations for fast and effective time series classification. *Data Mining and Knowledge Discovery* (2022), 1–24.
- [83] Wensi Tang, Guodong Long, Lu Liu, Tianyi Zhou, Michael Blumenstein, and Jing Jiang. 2021. Omni-Scale CNNs: a simple and effective kernel size configuration for time series classification. In *International Conference on Learning Representations*.
- [84] Erico Tjoa and Cuntai Guan. 2020. A survey on explainable artificial intelligence (xai): Toward medical xai. *IEEE transactions on neural networks and learning systems* 32, 11 (2020), 4793–4813.
- [85] Yongxin Tong, Xuchen Pan, Yuxiang Zeng, Yexuan Shi, Chunbo Xue, Zimu Zhou, Xiaofei Zhang, Lei Chen, Yi Xu, Ke Xu, et al. 2022. Hu-Fu: efficient and secure spatial queries over data federation. *Proceedings of the VLDB Endowment* 15, 6 (2022), 1159.
- [86] Paul Voigt and Axel Von dem Bussche. 2017. The eu general data protection regulation (gdpr). *A Practical Guide, 1st Ed., Cham: Springer International Publishing* 10, 3152676 (2017), 10–5555.
- [87] Yansheng Wang, Yongxin Tong, Dingyuan Shi, and Ke Xu. 2021. An efficient approach for cross-silo federated learning to rank. In *2021 IEEE 37th International Conference on Data Engineering (ICDE)*. IEEE, 1128–1139.
- [88] Kang Wei, Jun Li, Ming Ding, Chuan Ma, Howard H Yang, Farhad Farokhi, Shi Jin, Tony QS Quek, and H Vincent Poor. 2020. Federated learning with differential privacy: Algorithms and performance analysis. *IEEE Transactions on Information Forensics and Security* 15 (2020), 3454–3469.
- [89] Yuncheng Wu, Shaofeng Cai, Xiaokui Xiao, Gang Chen, and Beng Chin Ooi. [n.d.]. Privacy Preserving Vertical Federated Learning for Tree-based Models. *Proceedings of the VLDB Endowment* 13, 11 ([n.d.]).
- [90] Ke Yan, Zhiwei Ji, Huijuan Lu, Jing Huang, Wen Shen, and Yu Xue. 2017. Fast and accurate classification of time series data using extended ELM: Application in fault diagnosis of air handling units. *IEEE Transactions on Systems, Man, and Cybernetics: Systems* 49, 7 (2017), 1349–1356.
- [91] Qiang Yang, Yang Liu, Tianjian Chen, and Yongxin Tong. 2019. Federated machine learning: Concept and applications. *ACM Transactions on Intelligent Systems and Technology (TIST)* 10, 2 (2019), 1–19.
- [92] Shengwen Yang, Bing Ren, Xuhui Zhou, and Liping Liu. 2019. Parallel distributed logistic regression for vertical federated learning without third-party coordinator. *arXiv preprint arXiv:1911.09824* (2019).
- [93] Andrew C Yao. 1982. Protocols for secure computations. In *23rd annual symposium on foundations of computer science (sfcs 1982)*. IEEE, 160–164.
- [94] Lexiang Ye and Eamonn Keogh. 2011. Time series shapelets: a novel technique that allows accurate, interpretable and fast classification. *Data mining and knowledge discovery* 22, 1-2 (2011), 149–182.
- [95] Chengliang Zhang, Suyi Li, Junzhe Xia, Wei Wang, Feng Yan, and Yang Liu. 2020. {BatchCrypt}: Efficient homomorphic encryption for {Cross-Silo} federated learning. In *2020 USENIX annual technical conference (USENIX ATC 20)*. 493–506.
- [96] Chen Zhang, Yu Xie, Hang Bai, Bin Yu, Weihong Li, and Yuan Gao. 2021. A survey on federated learning. *Knowledge-Based Systems* 216 (2021), 106775.
- [97] Wenting Zheng, Ryan Deng, Weikeng Chen, Raluca Ada Popa, Aurojit Panda, and Ion Stoica. 2021. Cerebro: A Platform for {Multi-Party} Cryptographic Collaborative Learning. In *30th USENIX Security Symposium (USENIX Security 21)*. 2723–2740.